International Atomic Energy Agency

INDC(CCP)-15/U
DEC.1971

INDC INTERNATIONAL NUCLEAR DATA COMMITTEE

USSR STATE COMMITEE ON THE UTILIZATION OF ATOMIC ENERGY NUCLEAR DATA INFORMATION CENTRE

Nuclear Physics Research in the USSR
(Collected abstracts)

No.10

English translation of an original in Russian
published by Atomizdat, 1970

IAEA NUCLEAR DATA SECTION, KÄRNTNER RING 11, P.O. BOX 590, A-1011 VIENNA

INDC(CCP)-15/U

USSR STATE COMMITTEE ON THE UTILIZATION OF ATOMIC ENERGY
NUCLEAR DATA INFORMATION CENTRE

Nuclear Physics Research in the USSR
(Collected abstracts)

No. 10

English translation of an original in Russian
published by Atomizdat, 1970

Institute of Physics and Power Engineering

RADIATIVE CAPTURE OF FAST NEUTRONS BY ^{232}Th NUCLEI IN THE ENERGY RANGE 0.01-15 MeV

A.V. Davletshin, V.A. Tolstikov,
A.I. Abramov

The authors make a critical analysis of experiments in which $\sigma(n,\gamma)$ for ^{232}Th, for neutrons with energies greater than 10 keV, was measured. In some instances the results are normalized to the reference cross-section values adopted at the present time. From their analysis of results presented in various publications, the authors derive a recommended curve for $\sigma(n,\gamma)$ ^{232}Th versus neutron energy in the 0.01- 14.5 MeV range.

Numerical data from the recommended curve

No.	Average energy, E_m keV	Recommended cross-section mbarn	No.	Average energy, E_m keV	Recommended cross-section mbarn
I	I2	962±I28	I9	900	I72 ± 6
2	I5	729± 62	20	I000	I35 ± 5
3	I8	692± 36	2I	II50	I32 ± 7
4	24	576± 22	22	2000	75,3 ± 3,7
5	30	532± 36	23	3000	27,8 ± 3,5
6	40	480± I6	24	4700	I8,I ± 3,0
7	50	399± 26	25	I4500	5,2 ± 0,8
8	60	345± 28			
9	75	299± I5			
I0	I00	275± 26			
II	I40	257± II			
I2	200	207± 6			
I3	300	I90± 7			
I4	400	I77± 7			
I5	500	I69± 5			
I6	600	I78± 6			
I7	700	I82± 8			
I8	800	I82± 7			

MEASUREMENT OF FISSION CROSS-SECTIONS FOR ^{235}U AND ^{239}Pu ON A NEUTRON SLOWING-DOWN-TIME SPECTROMETER

A.E. Samsonov, Yu.Ya. Stavissky, V.A. Tolstikov,
V.B. Chelnokov

(Submitted to Atomnaja Energija)

The authors measured fission cross-sections for ^{235}U and ^{239}Pu over the energy range 0.1 eV to 40 keV in lead, using a slowing-down-time spectrometer. The relative fission cross-section values were normalized on the basis of thermal fission cross-sections by additional measurements in a graphite prism placed beside the principal lead slowing-down prism. From the results of the measurements the authors plotted the ratios between the ^{239}Pu fission cross-sections and the ^{235}U fission cross-sections. The results are shown in Tables I-III.

Table I

Fission cross-sections for ^{235}U

E, eV	σ_f, barn	E, eV	σ_f, barn	E, eV	σ_f, barn
43500	I,84±0,I4	370	I3,97±0,56	24,5	4I,5±I,7
28I00	2,07±0,I3	3I0	I5,50±0,62	22,5	47,6±I,9
I9700	2,33±0,I3	265	I8,22±0,73	20,0	53,5±2,I
I3900	2,55±0,I3	220	20,05±0,80	I8,0	50,2±2,0
II200	2,80±0,I4	I85	I9,57±0,78	I6,5	46,5±I,9
8840	3,0I±0,I4	I65	20,05±0,80	I5,0	42,2±I,7
7I80	3,28±0,I5	I45	2I,32±0,85	I4,2	42,3±I,7
59 40	3,55±0,I5	I25	20,53±0,82	I2,5	45,3±I,8
4700	4,00±0,I6	I05	22,II±0,88	II,0	49,4±2,0
3600	4,6I±0,I8	9I,0	24,20±0,97	9,90	58,0±2,3
2570	5,35±0,2I	80,0	26,7 ±I,I	8,80	65,5±2,6
I970	6,24±0,24	69,0	30,I ±I,2	7,90	54,2±2,2
I660	6,88±0,27	62,0	34,9 ±I,4	7,20	39,7±I,6
I400	7,56±0,28	57,0	38,9 ±I,6	6,70	3I,6±I,3
II70	8,I3±0,33	5I,0	44,0 ±I,8	5,50	29,7±0,8
950	8,66±0,35	45,6	44,4 ±I,8	6,I0	25,I±I,0
800	9,88±0,39	40,0	42,2 ±I,7	4,70	I4,05±0,56
700	I0,58±0,43	35,5	46,9±I,9	4,I0	I7,37±0,70
580	II,75±0,47	3I,0	45,4 ±I,8	3,60	25,I±I,0
460	I2,26±0,49	27,5	4I,5 ±I,7	3,I5	30,5±I,2

E, eV	σ_f, barn	E, eV	σ_f, barn
2,70	28,7±I,I	0,53	I05±6
2,40	23,9±I,0	0,48	II9±8
2,I0	22,8±I,0	0,43	I34±II
I,73	30,3±I,2	0,37	I57±I4
I,45	44,7±I,8	0,34	I68±I7
I,26	58,4±2,3	0,3I	I78±I8
I,I0	72,5±2,9	0,27	I89±I9
0,98	79,6±3,2	0,23	I94±20
0,90	80,I±3,2	0,I9	207±2I
0,78	80,I±3,2	0,I6	239±24
0,68	84,5±3,4	0.II	282±28
0,60	94,5±4,7		

Table II

Fission cross-sections for ^{239}Pu

E, eV	σ_f, barn	E, eV	σ_f, barn	E, eV	σ_f, barn	E, eV	σ_f, barn
43500	I,4I±0,II	I970	3,3I±0,I3	265	I5,02±0,60	57,0	5I,6±2,I
28I00	I,44±0,I0	I660	3,94±0,I6	220	I6,55±0,66	5I,0	40,6±I,7
I9700	I,54±0,09	I400	4,54±0,I8	I85	I6,62±0,66	45,6	28,I±I,I
I3900	I,65±0,09	II70	5,42±0,22	I65	I6,57±0,66	40,0	I8,0±0,7
II200	I,72±0,08	950	5,75±0,23	I45	I7,42±0,70	35,5	I3,30±0,53
8840	I,85±0,08	800	5,86±0,24	I25	I9,68±0,79	3I,0	I3,60±0,55
7I80	I,97±0,08	700	6,20±0,25	I05	26,0 ±I,0	27,5	2I,90±0,88
5940	2,I4±0,09	580	7,88±0,32	9I,0	37,2±I,5	24,5	32,8±I,3
4700	2,33±0,09	460	9,43±0,38	80,0	45,9 ±I,9	22,5	39,3±I,6
3600	2,53±0,I0	370	9,6I±0,39	69,0	53,2 ±2,I	20,0	47,2±I,9
2570	2,80±0,II	3I0	II,87±0,48	62,0	54,0 ±2,2	I8,0	56,I±2,2

E, ev	σ_f, barn	E, eV	σ_f, barn	E, eV	σ_f, barn
I6,5	66,9±2,7	3,80	I3,0±0,5	0,63	I79±8,2
I5,0	8I,2±3,2	3,35	I4,6±0,6	0,56	25I±I4
I3,4	97,5±3,9	2,90	I6,8±0,7	0,50	348±23
II,7	I07±4	2,55	I9,5±0,8	0,46	465±35
I0,5	I0I±4	2,25	22,I±0,9	0,39	726±62
9,4	75,3±3,I	I,92	25,4±I,I	0,36	907±86
8,2	60,8±2,5	I,58	34,8±I,4	0,33	I075±I07
7,5	5I,2±2,I	I,38	4I,9±I,7	0,29	I250±I25
6,9	38,6±I,6	I,I5	52,7±2,I	0,25	I300±I30
6,4	28,4±I,I	I,05	62,0±2,5	0,2I	I220±I22
5,9	I6,4±0.7	0,95	72,3±2,9	0,I7	I045±I04
5,0	I2,0±0,5	0,84	88,4±3,5	0,I3	820±82
4,40	I2,0±0,5	0,73	I23 ±5,0	0,II	745±75

Table III

Fission cross-section ratios, σ_f $^{239}Pu/\sigma_f$ ^{235}U

E, eV	σ_f $^{239}Pu/\sigma_f$ ^{235}U	E, eV	σ_f $^{239}Pu/\sigma_f$ ^{235}U	E, eV	σ_f $^{239}Pu/\sigma_f$ ^{235}U
43500	0,763±0,086	3I00	0,537±0,03I	460	0,767±0,043
43600	0,726±0,072	2570	0,522±0,030	420	0,7I5±0,04I
28I00	0,69I±0,63	2220	0,5I9±0,30	370	0,687±0,040
23300	0,669±0,057	I970	0,529±0,030	340	0,7I3±0,04I
I9700	0,657±0,054	I790	0,530±0,030	3I0	0,76I±0,043
I6400	0,664±0,050	I660	0,570±0,032	285	0,780±0,044
I3900	0,643±0,046	I500	0,604±0,034	265	0,823±0,047
I2300	0,627±0,043	I400	0,599±0,034	245	0,848±0,048
II200	0,6II±0,040	I250	0,636±0,036	220	0,823±0,047
9900	0,6II±0,040	II70	0,666±0,038	200	0,840±0,048
8840	0,6I5±0,040	I070	0,666±0,038	I85	0,846±0,048
7940	0,596±0,039	950	0,663±0,038	I75	0,8I8±0,047
7I80	0,599±0,037	880	0,640±0,036	I65	0,820±0,047
6500	0,598±0,036	800	0,590±0,034	I55	0,826±0,047
5940	0,603±0,035	760	0,570±0,033	I45	0,847±0,048
5200	0,60I±0,034	700	0,585±0,034	I35	0,875±0,050
4700	0,580±0,033	640	0,625±0,036	I25	0,9I6±0,052
4I00	0,575±0,032	580	0,668±0,038	II5	I,043±0,059
3600	0,548±0,03I	520	0,775±0,043	I05	I,I75±0,067

DIFFERENTIAL CROSS-SECTIONS FOR NEUTRON SCATTERING AT SMALL ANGLES AND NEUTRON POLARIZABILITY

G.V. Anikin, I.I. Kotukhov

(Submitted to Jadernaja Fizika)

The authors publish measured neutron scattering cross-sections over a range of angles from 2.5 to 25°. The measurements were made in a reactor beam for six neutron energy spectra. The mean spectral energies and their form factors are shown in Table I as a six-group approximation.

Table I

$\bar{E}$ of spectrum, MeV	Spectral group energy (MeV) and weight (%, in brackets)					
0,575	0,5I0(42,I)	0,590(34,6)	0,690(I7,5)	0,770(3,7)	0,820(I,5)	0,875(0,6)
I,33	I,I9(29,2)	I,34(44,6)	I,50(I2,9)	I,60(7,8)	I,70(3,7)	I,83(I,8)
2,45	2,I7(36)	2,47(45,5)	2,78(I0,8)	2,98(5,5)	3,I8(I,2)	3,40(I,0)
4,5	3,85(39,2)	4,65(36,5)	5,63(I5)	6,65(6,I)	7,65(2,2)	8,8(I,0)
5,6	4,72(35,9)	5,87(39,4)	7,20(I3,4)	8,I5(7,3)	9,I5(3,2)	I0,2(0,8)
8,4	7,52(I7)	8,25(54)	9,05(20,6)	I0,2(5,6)	II,I(2)	I2,4(0,8)

The angular distributions of the neutrons were measured for three elements: uranium, lead and copper. Only relative differential cross-sections were obtained in the experiments. The absolute cross-sections in barns per steradian, shown in Table II, were derived by fitting the experimental points to theoretical curves calculated from an optical model. Analysis of the angular distributions shows that by assuming neutron polarizability of the order of 2×10^{-40} cm^3 one can appreciably improve the agreement between calculated and measured neutron angular distributions.

Table II

Differential cross-sections $\sigma(\vartheta)$, b/sr

Element	Copper					Lead					Uranium					
$\vartheta^{\circ}_{l.s.}$ \ $\bar{E}_n$, MeV	I,33	2,45	4,5	5,6	8,4	I,33	2,45	4,5	5,6	8,4	0,575	I,33	2,45	4,5	5,6	8,4
2,5	0,554	0,8I3	2,05	2,67	3,45	2,I4	4,2I	7,29	9,45	II,I2	2,II	2,45	4,49	8,28	9,I9	9,79
3,I5	0,543	0,847	I,99	2,55	3,55	2,I7	4,I7	7,I7	9,43	I0,76	I,80	2,35	4,45	8,09	9,06	9,43
4,8	0,538	0,8II	2,0I	2,6I	3,26	I,99	4,05	6,98	8,87	I0,52	I,73	2,24	4,28	7,87	8,30	8,67
6,75	0,535	0,8I3	I,96	2,43	3,II	2,0I	3,94	6,65	8,64	9,85	I,52	2,I8	4,I0	7,39	8,I6	7,64
9,05	0,536	0,776	I,90	2,45	2,86	I,93	3,74	6,09	7,93	8,23	I,57	2,I4	3,90	6,87	7,47	6,92
I0,7	0,528	0,765	I,85	2,2I	2,79	I,86	3,6I	5,85	7,58	7,32	I,44	2,I0	3,80	6,49	7,05	6,I5
I2,3	0,523	0,754	I,72	2,2I	2,5I	I,86	3,55	5,52	7,07	6,I5	I,36	2,03	3,66	6,0I	6,39	5,I8
I4,0	0,5I7	0,748	I,64	2,07	2,47	I,84	3,35	4,97	6,43	5,6I	I,34	I,98	3,50	5,52	5,74	4,52
I5,6	0,505	0,704	I,60	2,07	2,20	I,8I	3,I8	4,75	5,98	4,9I	I,26	I,97	3,28	5,00	5,36	3,89
I7,25	0,50I	0,680	I,45	I,83	2,02	I,76	3,07	4,22	5,33	3,89	I,33	I,95	3,II	4,42	4,67	3,22
I8,I	0,489	0,666	I,47	I,77	I,98	I,68	2,95	3,98	5,I4	3,4I	I,27	I,87	2,99	4,22	4,22	2,89
I8,9	0,492	0,637	I,39	I,78	I,98	I,65	2,95	3,8I	4,86	3,I0	I,3I	I,85	2,85	3,95	3,98	2,56
I9,7	0,494	0,66I	I,36	I,66	I,87	I,67	2,77	3,62	4,23	2,77	I,26	I,77	2,7I	3,84	3,77	2,I4
20,55	0,499	0,634	I,3I	I,5I	I,73	I,62	2,73	3,45	4,II	2,50	I,I7	I,80	2,62	3,58	3,46	I,89
2I,35	0,49I	0,65I	I,25	I,42	I,62	I,6I	2,64	3,26	3,90	I,97	I,I0	I,73	2,5I	3,27	3,I8	I,70
22,2	0,476	0,578	I,I8	I,47	I,49	I,54	2,55	3,07	3,62	I,98	I,09	I,69	2,39	3,08	3,04	I,5I
23,8	0,458	0,547	I,I0	I,35	I,30	I,47	2,3I	2,73	3,06	I,4I	I,I0	I,65	2,24	2,67	2,52	I,I3

MEASUREMENT OF $\bar{\nu}$ IN FAST NEUTRON INDUCED FISSION OF ^{235}U AND EVALUATION OF THE DATA

L.I. Prokhorova, R.E. Bagdasarov, I.I. Kotukhov, V.G. Nesterov, B. Nurpeisov, G.N. Smirenkin, Yu.M. Turchin

(Submitted to Atomnaja Energija)

The authors employ a relative method to measure the average number of prompt neutrons ($\bar{\nu}$) emitted per fission event in uranium-235 as a function of bombarding neutron energy (E_n) over the range 0-1.5 MeV. As a reference value they used $\bar{\nu}$ for spontaneous fission of californium-252. A neutron detector consisting of 24 ^3He counters immersed in a paraffin block was used. The detector has an efficiency of ~ 20% and is characterized by a mean neutron lifetime of ~ 50 μsec. The resulting data, accurate to within 0.8-1%, indicate substantial deviations from a linear dependence. From an analysis of all the published data the authors derive a recommended curve for $\bar{\nu}(E_n)$.

The results of the measurements are shown in Table I, which gives the mean value and spread of the neutron energies $E_n \pm \Delta E_n$ and $\bar{\nu}(E_n)$. The frequently used value $\bar{\nu}$ (^{252}Cf) = 3.782 is taken as a convenient standard for comparisons with other data.

In Fig. 1 the values of $\bar{\nu}$ obtained for ^{235}U (black dots) are compared with results obtained by other authors in experiments with monoenergetic neutrons (accurate to within at least 2%). The sources and symbols are given in Ref. [1].

A qualitative study of the results shown in Fig. 1 indicates that despite the considerable spread of the experimental data the points are grouped around a mean path of intricate shape. To throw more light on the path of the curve we propose to consider a few examples selected from the full range of experimental data, giving preference to the most detailed measurements.

Many of the points on the low-energy segment of the $\bar{\nu}(E_n)$ curve are based on data in Refs [2, 3, 4], obtained at the Institute of Physics and Power Engineering in 1961. Table II contains a summary of the data presented in these papers. In converting the relative measurements of $\bar{\nu}(E_n)/\bar{\nu}_{therm}$ given in Table II to absolute values we adopted $\bar{\nu}_{therm}$ (^{235}U) = 2.418 ± 0.005, which corresponds to the value of $\bar{\nu}$ recommended in Ref. [5].

Figure 2 shows data taken from Refs [1, 2, 3, 4, 6, 7, 8]. Here the data from Ref. [6], which were measured with the highest energy resolution and which show sharp fluctuations in the narrow region E_n = 0.30-0.42 MeV (see Fig. 1), have been averaged (over three points: 0.298, 0.325 and 0.358 MeV, and 0.375,

0.405 and 0.425 MeV, respectively) for convenience of comparison with other data having poorer energy resolution. The data shown in Fig. 2 tally quite satisfactorily and clearly indicate the "step" in the $\bar{\nu}$ curve in the energy range 0.2–0.7 MeV. The step-like variation of $\bar{\nu}(E_n)$ at higher energies shows up equally clearly in the two most detailed measurements [3, 8].

The top part of Fig. 3 is a histogram of $<\bar{\nu}>$ values obtained by averaging the data in Fig. 2 over the region $E_n < 3.5$ MeV, for which sufficiently detailed experimental information is available. The averaging was carried out over the narrow energy intervals ΔE_n = 0.1 MeV ($0 < E_n < 1.2$ MeV) and 0.2 MeV ($1.2 < E_n < 3.4$ MeV) with weights inversely proportional to the squares of the errors in σ. Apart from the values of $<\bar{\nu}>$, Table III shows the errors

$$\sigma_I = \sqrt{\frac{\sum (\bar{\nu}_i - <\bar{\nu}>)^2 \frac{1}{\sigma_i^2}}{(n-1)\sum \frac{1}{\sigma_i^2}}} \quad \text{and} \quad \sigma_{II} = \frac{1}{\sqrt{\sum \frac{1}{\sigma_i^2}}}$$

the first of which reflects the spread of $\bar{\nu}_i$ values within a given interval ΔE_n, while the second indicates the accuracy of the general mean $<\bar{\nu}>$, given the condition that the averaged values are consistent.

The broken line in Fig. 3 is the smooth curve of $\bar{\nu}(E_n)$ for ^{235}U recommended by us, which is also reflected by Table III and below 2 MeV conforms fairly closely with the histogram for $<\bar{\nu}>$. At $E_n > 2$ MeV the recommended curve contains, for the reasons given, a large element of chance. But, as can be seen from the histogram at the bottom of Fig. 3, the inaccuracies caused thereby are not of great practical importance. The lower histogram shows the limits of permissible errors in the group constants $\frac{\delta<\bar{\nu}>}{<\bar{\nu}>}$, as evaluated in Ref. [9], when the multiplication constant $\frac{\Delta K_{eff}}{K_{eff}} = \pm 1\%$ and the breeding ratio $\frac{\Delta KB}{KB} = \pm 2\%$ are calculated with a given accuracy for different commercial-scale fast breeder reactors. These are derived on the assumption that the sources of error in the different constants are independent. The arrows indicate the boundaries of the energy groups for which $\frac{\delta<\bar{\nu}>_c}{<\bar{\nu}>_c}$ has the indicated values, while the dots show the relative errors in $\frac{\delta<\bar{\nu}>}{<\bar{\nu}>}$ corresponding to the largest values of σ_1 and σ_2 shown in Table III: $\delta<\bar{\nu}> \equiv \max(\sigma_I, \sigma_{II})$.

The histogram shown in Fig. 3 for $\frac{\delta<\bar{\nu}>_c}{<\bar{\nu}>_c}$ was calculated in Ref. [9] for reactors using plutonium-239 rather than uranium-235 as fuel, but this difference is unimportant for evaluating the comparative requirements imposed on the accuracy of $\bar{\nu}_i$ measurements in various neutron energy regions.

Above 3.5 MeV the recommended curve in Fig. 3 corresponds to the following expressions:

$$\bar{\nu}(E_n) = \begin{cases} 2.395 + 0.127\, E_n & 3.5 < E_n < 5.0 \text{ MeV} \quad (1) \\ 2.028 + 0.200\, E_n & 5.0 < E_n < 7.5 \text{ MeV} \quad (2) \\ 2.485 + 0.139\, E_n & 7.5 < E_n < 16 \text{ MeV} \quad (3) \end{cases}$$

Expression (1) was obtained by the method of least square deviations of the experimental data on $\bar{\nu}$ for uranium-235 in the range 1.2-5 MeV. Expressions (2) and (3) are from Ref. [10].

Table I

Measurements of $\bar{\nu}$ for uranium-235 in the present paper

E_n (MeV)	$\bar{\nu}(E_n)$
0,00	2,4I2 ± 0,0I4
0,080	2,404 ± 0,039
0,2I4 ± 0,040	2,467 ± 0,020
0,322 ± 0,043	2,457 ± 0,020
0,408 ± 0,042	2,474 ± 0,024
0,5I0 ± 0,039	2,484 ± 0,027
0,686 ± 0,039	2,452 ± 0,025
0,8I0 ± 0,038	2,5I4 ± 0,020
0,9I0 ± 0,037	2,5I8 ± 0,026
I,002 ± 0,062	2,558 ± 0,025
I,II2 ± 0,035	2,578 ± 0,022
I,3I4 ± 0,035	2,574 ± 0,024
I,5I5 ± 0,035	2,572 ± 0,025

Table II

Measurements of $\bar{\nu}$ for uranium-235 made at the Institute of Physics and Power Engineering

Reference	E_n (MeV)	$\bar{\nu}/\bar{\nu}_{therm}$	$\bar{\nu}(E_n)$
[2]	0,08	I,000 ± 0,0I2	2,4I8 ± 0,030
	0,08	0,984 ± 0,0I5	2,379 ± 0,035
	0,I9 ± 0,09	I,007 ± 0,0I6	2,436 ± 0,038
	0,29 ± 0,04	I,022 ± 0,0I4	2,470 ± 0,034
	0,3I ± 0,04	I,02I ± 0,0I0	2,468 ± 0,025
	0,39 ± 0,05	I,025 ± 0,007	2,478 ± 0,0I7
	0,46 ± 0,05	I,026 ± 0,0I5	2,480 ± 0,037
	0,55 ± 0,05	I,009 ± 0,0I0	2,438 ± 0,024
	0,64 ± 0,05	I,0I6 ± 0,0I5	2,455 ± 0,038
	0,67 ± 0,05	I,024 ± 0,009	2,475 ± 0,023
	0,78 ± 0,06	I,023 ± 0,0I0	2,473 ± 0,025
	0,99 ± 0,06	I,037 ± 0,0I2	2,507 ± 0,029
[3]	0,59 ± 0,I0	I,024 ± 0,0I4	2,475 ± 0,035
	0,8I ± 0,09	I,020 ± 0,0I4	2,466 ± 0,035
	I,02 ± 0,08	I,052 ± 0,0II	2,543 ± 0,027
	I,23 ± 0,08	I,059 ± 0,0I5	2,560 ± 0,037
	I,44 ± 0,07	I,062 ± 0,0I5	2,588 ± 0,037
	I,64 ± 0,07	I,072 ± 0,0I5	2,592 ± 0,036
	I,85 ± 0,07	I,084 ± 0,0I4	2,622 ± 0,034
	2,05 ± 0,06	I,079 ± 0,0I3	2,6I0 ± 0,03I
	2,25 ± 0,06	I,I09 ± 0,0I5	2,682 ± 0,037
	2,46 ± 0,06	I,I43 ± 0,0I7	2,763 ± 0,042
	2,76 ± 0,06	I,I66 ± 0,0I6	2,820 ± 0,038
	3,06 ± 0,05	I,I70 ± 0,0I8	2,830 ± 0,050
	3,25 ± 0,05	I,I82 ± 0,0I9	2,857 ± 0,046
[4]	0,08	I,0II ± 0,0I0	2,444 ± 0,024
	0,20 ± 0,05	I,038 ± 0,0I0	2,5II ± 0,025
	0,30 ± 0,05	I,033 ± 0,009	2,498 ± 0,023
	0,50 ± 0,05	I,023 ± 0,009	2,473 ± 0,022
	0,60 ± 0,05	I,020 ± 0,009	2,466 ± 0,02I
	0,70 ± 0,05	I,0I9 ± 0,009	2,464 ± 0,022

Table III

Recommended average values of $\bar{\nu}$ for uranium-235

E_n (MeV)	$< \bar{\nu} >$	σ_I	σ_{II}	$\bar{\nu}(E_n)$ */
0 - 0,1	2,423	0,005	0,007	2,425
0,1 - 0,2	2,455	0,010	0,014	2,455
0,2 - 0,3	2,471	0,006	0,007	2,472
0,3 - 0,4	2,475	0,010	0,007	2,481
0,4 - 0,5	2,493	0,011	0,008	2,486
0,5 - 0,6	2,485	0,010	0,009	2,485
0,6 - 0,7	2,485	0,009	0,008	2,485
0,7 - 0,8	2,488	0,016	0,009	2,488
0,8 - 0,9	2,502	0,009	0,010	2,501
0.9 - 1,0	2,512	0,007	0,010	2,515
1,0 - 1,1	2,549	0,007	0,010	2,547
1,1 - 1,2	2,555	0,011	0,011	2,558
1,2 - 1,4	2,564	0,010	0,011	2,566
1,4 - 1,6	2,591	0,007	0,010	2,586
1,6 - 1,8	2,609	0,014	0,015	2,609
1,8 - 2,0	2,638	0,007	0,010	2,636
2,0 - 2,2	2,671	0,019	0,020	2,673
2,2 - 2,4	2,716	0,020	0,023	2,706
2,4 - 2,6	2,702	0,011	0,010	2,736
2,6 - 2,8	2,788	-	0,022	2,764
2,8 - 3,0	2,756	0,016	0,009	2,786
3,0 - 3,2	2,814	-	0,027	2,806
3,2 - 3,4	2,848	-	0,029	2,826

*/ The last column gives values of $\bar{\nu}(E_n)$ corresponding to the smooth recommended curve for the middle of the energy interval. Above 3.5 MeV this corresponds to expressions (3) and (4).

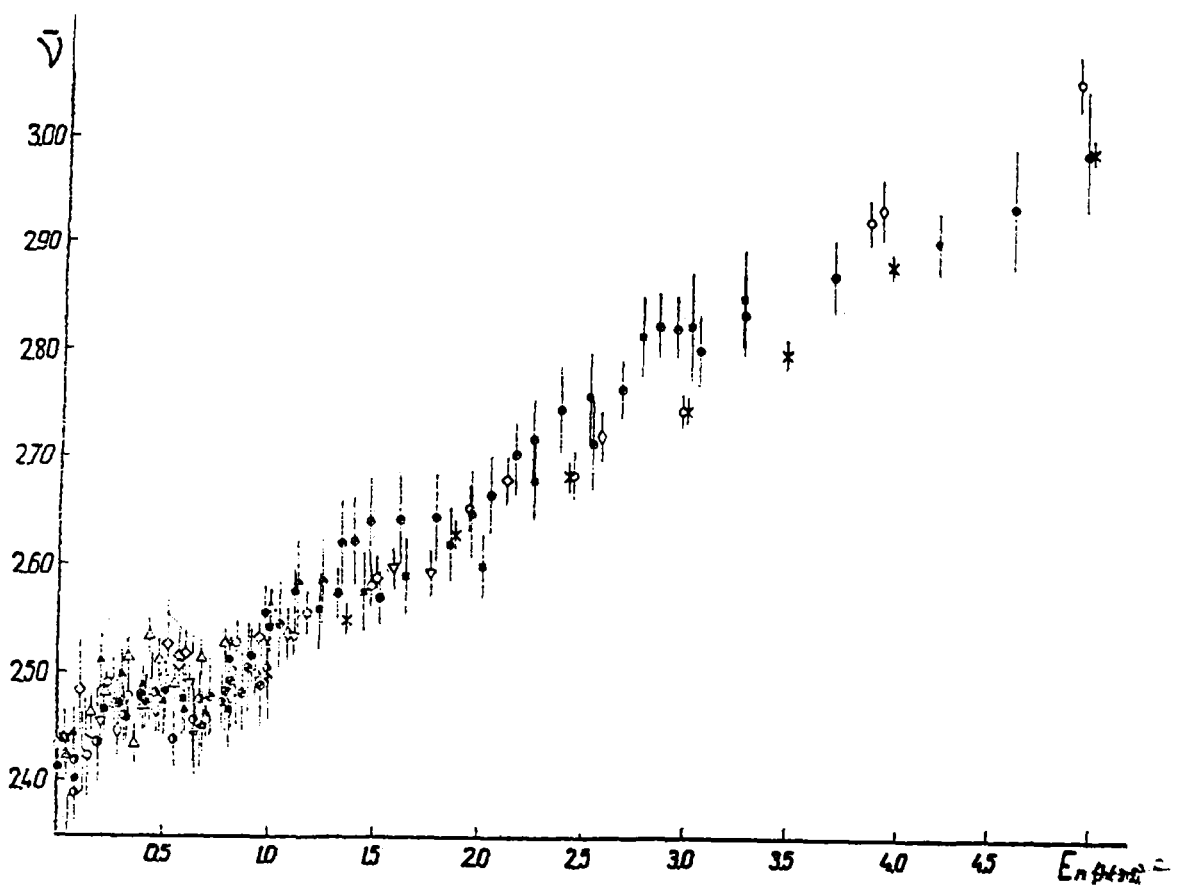

Fig. 1 Complete data on average number of prompt neutrons $\bar{\nu}$ for uranium-235 ($E_n \leq 5$ MeV) (see text).

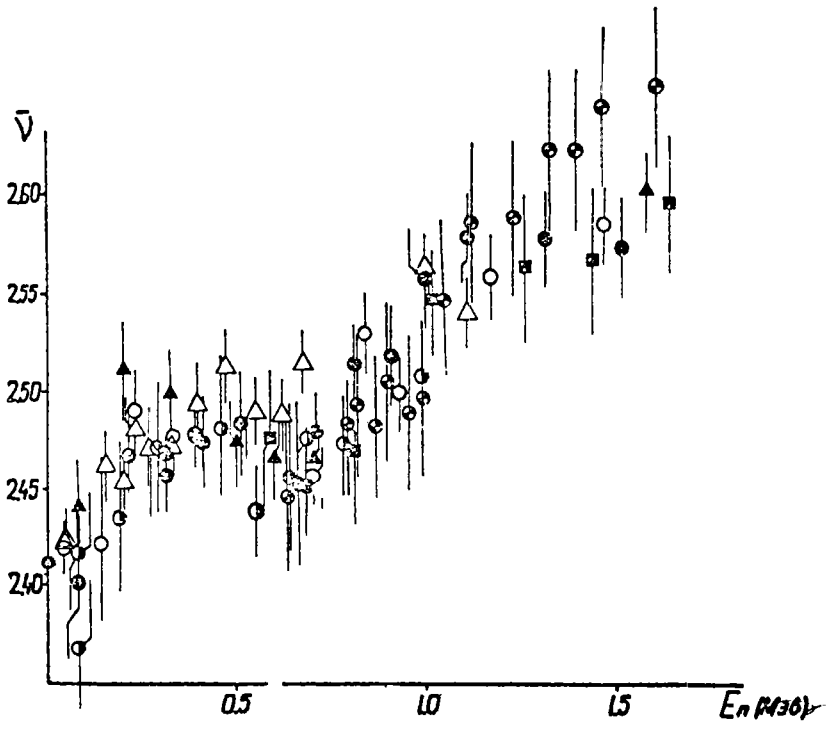

Fig. 2 Selected data from the most detailed measurements of $\bar{\nu}$

▲ - [4]; ◐ - [2]; ■ - [3]

△ - [6]; 0 - [7]; ● - present paper.

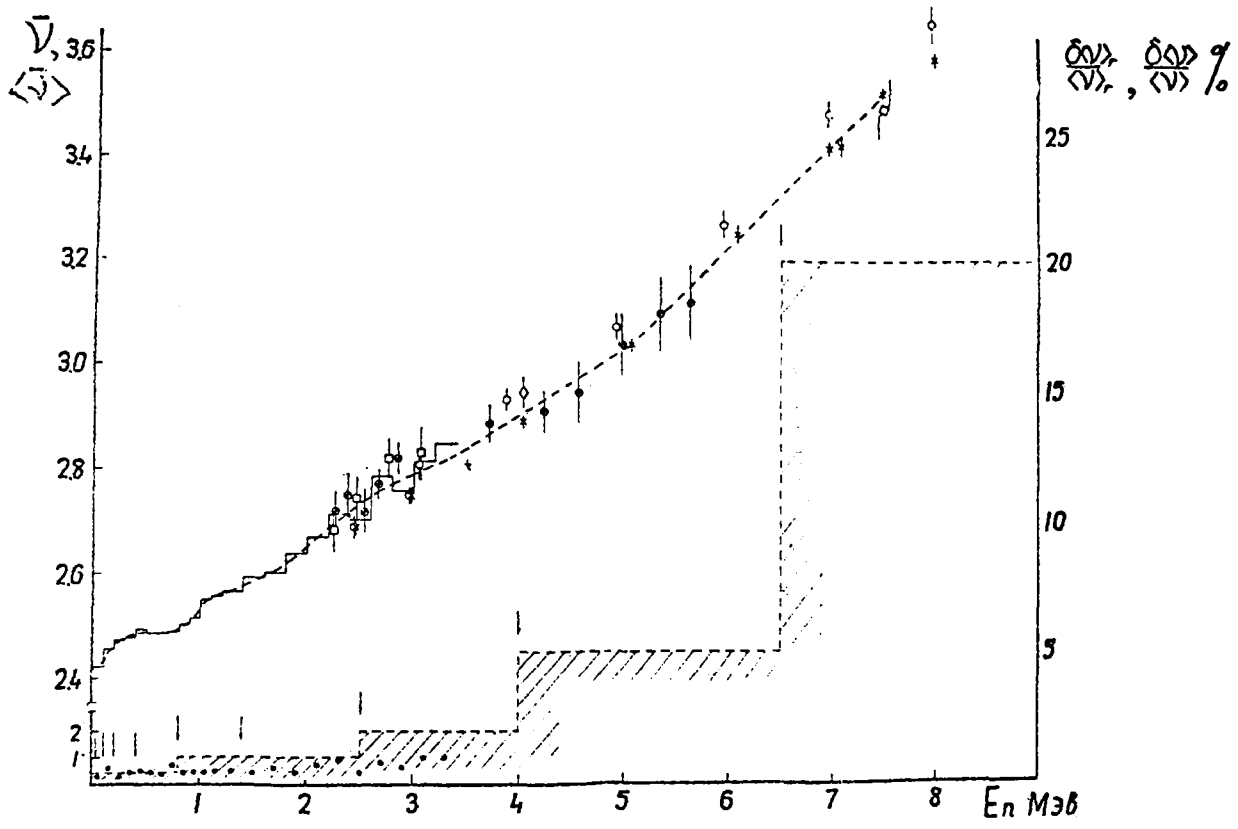

Fig. 3 Above: Different versions of an average description of experimental data for $\bar{\nu}(E_n)$. Below: Limits of permissible accuracy for the group constants $\frac{\delta < \bar{\nu} >_c}{< \bar{\nu} >_c}$ (histogram and accuracy obtained in relative measurements of $\frac{\delta < \nu >}{< \nu >}$ (dots), see text).

REFERENCES

[1] PROKHOROVA, L.I., BAGDASAROV, R.E., KOTUKHOV, I.I., NESTEROV, V.G., NURPEISOV, B., SMIRENKIN, G.N., TURCHIN, Yu.M., Atomnaja energija (in press).

[2] BLJUMKINA, Yu.A., BONDARENKO, I.I., KUZNETSOV, V.F., NESTEROV, V.G., OKOLOVICH, V.N., SMIRENKIN, G.N., USACHEV, L.N., Nucl. Phys. 52 (1964) 648.

[3] PROKHOROVA, L.I., SMIRENKIN, G.N., Jadernaja fizika 7 (1968) 961.

[4] KUZNETSOV, V.F., SMIRENKIN, G.N., Nuclear data for reactors (Proc. Symp. Paris 1966) 2, IAEA, Vienna (1967) 75.

[5] FILMORE, F.L., J. Nucl. Energy 22 (1968) 79.

[6] MEADOWS, J.W., WHALEN, J.F., J. Nucl. Energy 21 (1967) 157.

[7] MATHER, D.S., FIELDHAUSE, P.F., MOAT, A., Phys. Rev. 133 (1964) B1403.

[8] SAVIN. M.V., KHOKHLOV, Yu.A., PARAMONOVA, I.N., ZAMYATNIN, Yu.S., Nuclear data for reactors (Proc. Symp. Helsinki 1970), IAEA, Vienna (1970)157.

[9] ZARITSKY, S.M., TROYANOV, M.F., Fizika jadern. reakt. (Physics of nuclear reactors) 2 Atomizdat (1970).

[10] SOLEILHAC, M., FREHAUT, I., GAURIAU, I. J. Nucl. Energy, 23 (1969) 257.

NEUTRON-INDUCED SUB-THRESHOLD FISSION OF PLUTONIUM-238

S.B. Ermagambetov, G.N. Smirenkin

(Submitted to Atomnaja Energija)

Using the T(p,n) reaction, the authors measured fission cross-sections for plutonium-238 fission by neutrons with E_n = 2.5 keV–2.5 MeV in an electrostatic generator. Well below the threshold at ~ 0.5 MeV, in the previously unstudied range $E_n \leqslant 0.05$ MeV the fission cross-section increases appreciably, attaining values close to 2 barns in the plateau region. Analysis of the low-energy section of the cross-section curve shows approximately the same probability of plutonium-238 fission by s and p neutrons.

Measurements of fission cross-sections (σ_f) for plutonium-238 and adopted reference values of σ_f for uranium-235

E_n, keV	σ_f (^{238}Pu), barn	σ_f (^{235}U), barn
2,4 ± I,3	I,70 ± 0,I8	5,45
5,5 ± 2,5	I,30 ± 0,I2	4,00
II,3 ± 6,0	0,83 ± 0,06	3,I3
I4,4 ± 5,0	0,88 ± 0,07	2,86
25,5 ± I0	0,55 ± 0,04	2,40
46,4 ± 20	0,62 ± 0,04	2,00
53 ± 6	0,52 ± 0,03	I,93
70 ± 7	0,50 ± 0,03	I,76
78 ± I0	0,47 ± 0,02	I,72
II0 ± 7	0,62 ± 0,03	I,60
I20 ± I0	0,53 ± 0,03	I,56
200 ± 20	0,60 ± 0,03	I,40
250 ± 5	0,80 ± 0,04	I,35
290 ± 20	0,84 ± 0,04	I,3I
305 ± I0	I,05 ± 0,05	I,29
350 ± 8	I,06 ± 0,04	I,26
420 ± I5	I,I4 ± 0,05	I,20
635 ± 25	I,60 ± 0,06	I,I3
680 ± 25	I,60 ± 0,06	I,I3

E_n, keV	σ_f (^{238}Pu), barn	σ_f (^{235}U), barn
770 ± 25	I,67 ± 0,07	I,I7
9I0 ± I0	2,06 ± 0,08	I,20
I080 ± 20	2,II ± 0,08	I,22
I2I0 ± 20	2,I3 ± 0,08	I,22
I330 ± 20	2,08 ± 0,08	I,22
I430 ± 25	2,20 ± 0,I0	I,22
I500 ± 20	2,I5 ± 0,07	I,23
I650 ± 20	2,20 ± 0,I0	I,25
I800 ± 20	2,I8 ± 0,I0	I,28
2000 ± 20	2,30 ± 0,I0	I,32
2260 ± 20	2,25 ± 0,09	I,3I
2400 ± 20	2,22 ± 0,09	I,28

ANGULAR ANISOTROPY AND FISSIONABILITY OF NUCLEI

G.N. Smirenkin, A.S. Tishin

(Submitted to Jadernaja Fizika)

The authors investigate, within the framework of statistical theory [1], the effect of nuclear fissionability on the angular anisotropy of fission. It is demonstrated that the dependence of fissionability on the total angular momentum must be taken into account in processing and compiling experimental data on the angular distribution of fission fragments.

Taking the example of fission of even-even target nuclei, the authors derive in a quasi-classical approximation [2] the following expression for the angular distribution of the fission fragments:

$$W(\theta) \sim \int_0^{J_{max}} \frac{J \exp(-J^2 \sin^2\theta/4K_0^2) I_0(J^2 \sin^2\theta/4K_0^2)\, dJ}{\Gamma_n(0)\exp(-\beta J^2) + \sqrt{\frac{\pi}{2}}\,\Gamma_f(0)\,\frac{K_0}{J}\,\mathrm{erf}(J/\sqrt{2}K_0)}, \quad (1)$$

in which the distribution of angular momenta depends on the relation

$$\frac{\Gamma_f(J)}{\Gamma_n(J)} = \sqrt{\frac{\pi}{2}}\,\frac{K_0}{J}\,\mathrm{erf}(J/\sqrt{2}K_0)\exp(\beta J^2)\,\frac{\Gamma_f(0)}{\Gamma_n(0)}, \quad (2)$$

where the parameter K_0^2 determines the distribution of the projections K of the total angular momentum J onto the axis of symmetry of the nucleus; $\Gamma_f(0)$ and $\Gamma_n(0)$ are the mean widths for fission and neutron emission at $J = 0$; $I_0(x)$ is the Bessel function for the imaginary argument, and erf(x) is the probability integral. The parameter $\beta = \alpha_n - \alpha_f$ with $\alpha_i = \hbar^2/2J_iT_i$, where J_i is the effective moment of intertia; T_i is the temperature of the nucleus, and the subscripts i = n,f correspond to the state of the nucleus after emission of a neutron and to the transient state at the saddle point.

The authors demonstrate that the familiar expressions employed in analysing angular distributions of fission fragments are special cases of the more general relationship in expression (1) and indicate their limits of applicability.

Attention is drawn to the fact that the results of processing experimental data in the case of low fissionability are extremely sensitive to the assumption that Γ_f/Γ_n is dependent on J. Thus,

the processing of data on fission induced by alpha particles and heavy ions requires the greatest caution. In this case the following expression emerges from expression (1):

$$\frac{W(0°)}{W(90°)} = \frac{\rho}{\delta}(e^{\delta}-1)\left[\int_0^{\rho} e^{(\frac{\delta}{\rho}-1)x} I_0(x)\,dx\right]^{-1}, \quad (\delta=\beta J_{max}^2, \rho=J_{max}^2/4K_0^2) \qquad (3)$$

which is compared with other approximations in relation to ^{209}Bi (α,f) fission.

REFERENCES

[1] PIK-PICHAK, G.A., Zh. eksp. teor. fiz. 36 (1959) 961.

[2] STRUTINSKY, V.M., Zh. eksp. teor. fiz. 39 (1960) 781; 40 (1961) 933.

ANGULAR DISTRIBUTIONS OF FISSION FRAGMENTS AND CHANNEL ANALYSIS OF NEUTRON-INDUCED FISSION OF THORIUM-232

S.B. Ermagambetov, G.N. Smirenkin

(Submitted to Atomnaja Energija)

For 18 energies over the neutron energy range 0.95-2.3 MeV the authors measured the angular distributions of fission fragments, $W(\vartheta)$, resulting from $^{232}Th(n,f)$ reaction, using an electrostatic generator for the purpose. The measurements were made by the glass (track) detector method. The experimental data are presented in the table in the form of the expansion coefficients

$$\frac{W(\vartheta)}{W(90^\circ)} = \sum_{n=o}^{3} a_{2n} P_{2n}(\cos\vartheta)$$

and the angular anisotropy coefficient $W(0^\circ)/W(90^\circ)$. Channel analysis is performed on the $W(\vartheta)$ and fission cross-section (σ_f) data.

The principal conclusions from the analysis are that:

(1) The nature of the energy dependences $W(\vartheta,En)$ and $\sigma_f(En)$ is incompatible with the concept of smooth penetrability of the Hill-Wheeler parabolic barrier;

(2) The experimental data can be satisfactorily interpreted within the framework of a double-hump barrier model;

(3) Large uncertainties affect the identification of the quantum characteristics K^π participating in the division of states, and these are characteristic not only of the particular nucleus but of channel analysis of the (n,f) reaction as a whole.

Angular anisotropy and coefficients for Legendre polynomial expansion of the angular distributions of thorium-232 fission fragments

E_n (MeV)	a_0	a_2	a_4	a_6	$\frac{W(0°)}{W(90°)}$
0,95 ± 0,05	I,059 ± 0,0II	0,30I ± 0,023	0,235 ± 0,028	- 0,0II ± 0,034	I,585 ± 0,060
I,00 ± 0,05	I,085 ± 0,0I2	0,3I5 ± 0,024	0,I90 ± 0,03I	- 0,002 ± 0,036	I,590 ± 0,06I
I,I0 ± 0,05	I,I6I ± 0,0II	0,480 ± 0,023	0,292 ± 0,030	0,097 ± 0,034	2,03I ± 0,064
I,I5 ± 0,05	I,204 ± 0,0I0	0,394 ± 0,020	0,088 ± 0,027	0,I28 ± 0,03I	I,8I5 ± 0,056
I,20 ± 0,04	I,2I3 ± 0,0I4	0,394 ± 0,028	-0,023 ± 0,036	0,023 ± 0,042	I,608 ± 0,066
I,25 ± 0,04	I,I02 ± 0,0I2	0,2I0 ± 0,023	0,0II ± 0,030	0,005 ± 0,034	I,328 ± 0,053
I,30 ± 0,02	I,068 ± 0,009	0,22I ± 0,0I8	0,044 ± 0,023	-0,083 ± 0,026	I,25I ± 0,039
I,35 ± 0,02	I,0I8 ± 0,009	0,0I2 ± 0,0I7	-0,096 ± 0,022	-0,074 ± 0,025	0,85? ± 0,030
I,40 ± 0,02	0,992 ± 0,0II	-0,00I ± 0,020	-0,I03 ± 0,027	-0,I50 ± 0,030	0,737 ± 0,032
I,450± 0,02	I,0I7 ± 0,006	-0,068 ± 0,0II	-0,I85 ± 0,0I4	-0,057 ± 0,0I5	0,707 ± 0,0I7
I,500± 0,02	I,068 ± 0,0II	-0,04I ± 0,02I	-0,300 ± 0,029	-0,079 ± 0,03I	0,648 ± 0,032
I,550± 0,02	I,008 ± 0,005	-0,2II ± 0,0I0	-0,347 ± 0,0I3	-0,05I ± 0,0I3	0,398 ± 0,0I0
I,600± 0,02	I,028 ± 0,003	-0,I63 ± 0,005	-0,369 ± 0,007	-0,09I ± 0,007	0,404 ± 0,005
I,650 ± 0,02	I,00I ± 0,007	-0,I44 ± 0,0I4	-0,26I ± 0,0I9	-0,079 ± 0,0I9	0,5I6 ± 0,0I8
I,700±0,02	I,075 ± 0,008	-0,06I ± 0,0I4	-0,287 ± 0,0I9	-0,006 ± 0,02I	0,72I ± 0,032
I,80 ± 0,02	0,990 ± 0,006	0,052 ± 0,0II	0,035 ± 0,0I5	-0,072 ± 0,0I6	I,005 ± 0,02I
2,00 ± 0,02	I,083 ± 0,005	0,247 ± 0,009	0,089 ± 0,0I2	-0,022 ± 0,0I4	I,398 ± 0,024
2,30 ± 0,02	I,I52 ± 0,006	0,325 ± 0,0I3	0,075 ± 0,0I7	0,056 ± 0,0I9	I,607 ± 0,030

ANGULAR ANISOTROPY AND TARGET NUCLEUS SPIN IN [n,f] REACTIONS

G.N. Smirenkin, D.L. Shpak, Yu.B. Ostapenko, B.I. Fursov

Using an electrostatic generator with neutron output at 150° to the direction of the accelerated proton beam and applying the glass detector technique, the authors made a detailed study of the angular anisotropy of uranium-233, uranium-235 and plutonium-239 fission as a function of bombarding neutron energy in the range below 0.74 MeV. The experimental data are used in analysing the influence of target nucleus spin, I_o, on the angular anisotropy of fission, A. The nature of the observed dependence A (E_n) can be qualitatively described in a satisfactory manner by a statistical theory of fission fragment angular distributions.

The table below shows the coefficient of angular anisotropy, $A = \frac{W(0^\circ)}{W(90^\circ)}$, as a function of neutron energy E_n.

Table

Angular anisotropy of fission fragments from uranium-233, uranium-235 and plutonium-239

E_n (MeV)	A		
	^{233}U	^{235}U	^{239}Pu
0,015 ± 0,015			0,025 ± 0,021
0,030 ± 0,015	-0,015 ± 0,021		
0,055 ± 0,015	0,031 ± 0,013	-0,042 ± 0,009	0,054 ± 0,015
0,080 ± 0,015		-0,012 ± 0,013	0,045 ± 0,013
0,105 ± 0,015	0,077 ± 0,012	-0,029 ± 0,014	0,063 ± 0,012
0,130 ± 0,015		-0,013 ± 0,008	0,108 ± 0,015
0,155 ± 0,015	0,078 ± 0,013	-0,016 ± 0,011	0,096 ± 0,016
0,180 ± 0,015		0,013 ± 0,009	0,148 ± 0,016
0,220 ± 0,015	0,101 ± 0,020	0,014 ± 0,008	0,142 ± 0,013
0,260 ± 0,015		0,024 ± 0,016	0,123 ± 0,017
0,300 ± 0,015		0,003 ± 0,008	0,127 ± 0,027
0,340 ± 0,015		0,032 ± 0,014	0,121 ± 0,013
0,380 ± 0,015		0,018 ± 0,008	0,121 ± 0,012
0,420 ± 0,015		0,036 ± 0,013	0,103 ± 0,011
0,460 ± 0,015		0,030 ± 0,012	0,157 ± 0,019
0,500 ± 0,015		0,088 ± 0,017	0,141 ± 0,012
0,540 ± 0,015		0,074 ± 0,012	0,149 ± 0,018
0,580 ± 0,015		0,094 ± 0,015	0,112 ± 0,009
0,620 ± 0,015		0,101 ± 0,013	0,132 ± 0,009
0,660 ± 0,015		0,093 ± 0,006	0,097 ± 0,016
0,700 ± 0,015		0,103 ± 0,015	0,098 ± 0,015
0,740 ± 0,015		0,078 ± 0,014	0,122 ± 0,020

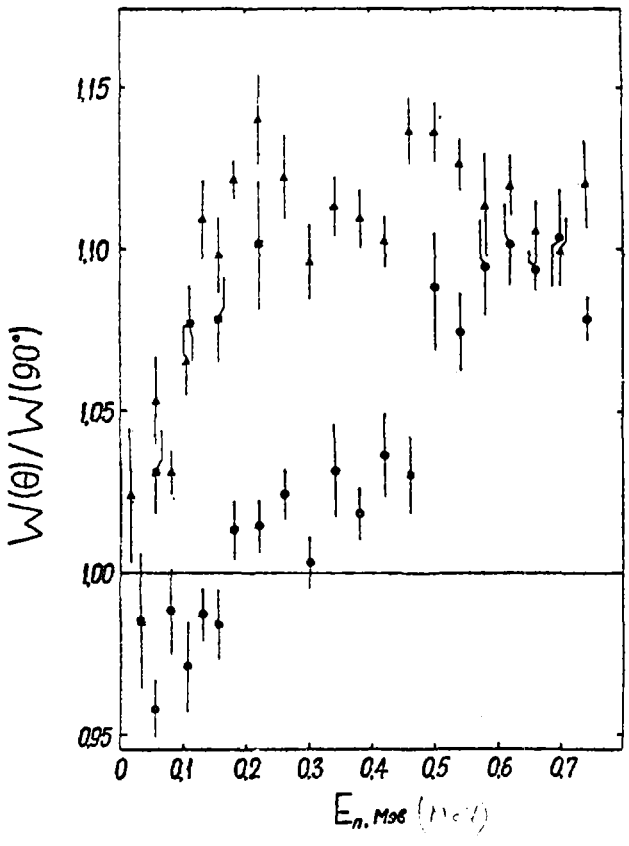

Fig. 1 Angular anisotropy of fission as a function of neutron energy: squares = ^{233}U; dots = ^{235}U; triangles = ^{239}Pu.

ANGULAR ANISOTROPY OF PLUTONIUM-239 PHOTOFISSION

A.S. Soldatov, Yu.M. Tsipenyuk*, G.N. Smirenkin

(Submitted to Jadernaja Fizika)

Using the microtron belonging to the Institute of Physical Problems (USSR Academy of Sciences), the authors studied the energy dependence of the fission cross-section σ_f and angular anisotropy, $A_\gamma = W(90^\circ)/W(0^\circ) - I$, of plutonium-239 photofission close to the threshold. The relevant data are shown in the figure. A combined analysis is made of the experimental data for the reactions $^{239}Pu(\gamma,f)$ and $^{238}Pu(n,f)$ [1]. The authors found a quasi-steady state of the dividing ^{239}Pu nucleus, $K^\pi = \frac{3^-}{2}$, at an excitation energy of 5.6 MeV (0.5 MeV below the barrier).

REFERENCE

[1] VOROTNIKOV, P.E., et al., Jad. fiz. 3 (1966) 479.

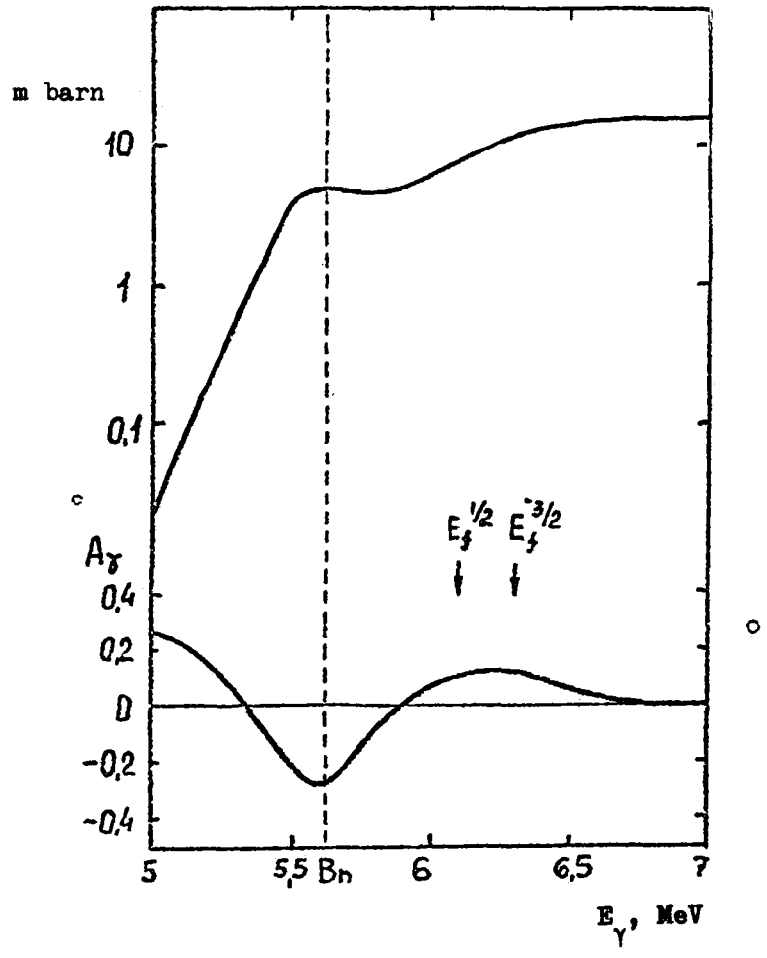

*/ Institute of Physical Problems, USSR Academy of Sciences, Moscow, USSR.

STATISTICAL ANALYSIS OF ANGULAR DISTRIBUTIONS OF FISSION FRAGMENTS IN NEUTRON-INDUCED FISSION OF URANIUM-238

Kh.D. Androsenko, G.N. Smirenkin, A.S. Tishin

The authors consider a variety of methods of processing the measured angular distributions of uranium-238 fission fragments in the neutron energy range 0.7-4 MeV. The T(p,n) and D(d,n) reactions were used to obtain monoenergetic neutrons. The angular distributions of the fragments were measured in two quadrants, 0-90° and 180-270°, relative to the direction of the beam, glass detectors being used for the purpose. The table contains the experimentally determined angular distributions and anisotropy values (from processing by Legendre polynomials).

The results of the processing are discussed from the standpoint of the consequences following from the double-hump barrier model. A description of the programme used to process the measured angular distributions - by the method of least squares, using the relationships of statistical theory - is attached.

$E_n \pm \Delta E_n$	$\frac{W(0°)}{W(90°)}$ $A \pm \Delta A$	W(5°)	W(12°)	W(20,5°)	W(30°)	W(40°)	W(50°)	W(60°)	W(70°)	W(80°)	W(88,5°)
0,700±0,05	I,395±0,013	I,364±0,04	I,371±0,04	I,356±0,04	I,233±0,03	I,159±0,03	I,094±0,03	I,038±0,03	I,024±0,03	0,988±0,03	I,000±0,03
0,800±0,05	I,366±0,016	I,362±0,05	I,328±0,04	I,259±0,04	I,146±0,04	I,080±0,04	I,087±0,04	I,011±0,04	I,022±0,04	I,024±0,04	I,000±0,04
0,900±0,05	I,396±0,03	I,446±0,08	I,462±0,07	I,344±0,07	I,279±0,06	I,266±0,06	I,275±0,06	I,204±0,06	I,146±0,06	I,088±0,06	I,000±0,06
0,935±0,03	I,499±0,03	I,476±0,07	I,508±0,07	I,341±0,06	I,321±0,06	I,265±0,06	I,084±0,05	I,028±0,05	0,976±0,05	0,978±0,05	I,000±0,06
I,05 ±0,05	I,367±0,02	I,351±0,03	I,278±0,03	I,241±0,03	I,192±0,03	I,127±0,03	I,063±0,03	I,008±0,03	0,965±0,03	0,954±0,03	I,000±0,03
I,15 ±0,04	I,316±0,02	I,320±0,04	I,249±0,03	I,219±0,03	I,194±0,03	I,126±0,03	I,118±0,03	I,095±0,03	I,037±0,03	I,015±0,03	I,000±0,03
I,20 ±0,04	I,602±0,02	I,606± 0,04	I,622±0,04	I,540±0,04	I,396±0,03	I,281±0,03	I,159±0,03	I,095±0,03	I,088±0,03	I,056±0,03	I,000±0,03
2,20 ±0,04	I,257±0,01	I,252±0,02	I,235±0,02	I,186±0,02	I,154±0,02	I,116±0,02	I,083±0,02	I,049±0,02	0,989±0,02	0,993±0,02	I,000±0,02
2,80 ±0,03	I,181±0,02	-	I,188±0,04	I,190±0,03	I,188±0,03	I,162±0,02	I,130±0,02	I,087±0,03	I,061±0,03	I,021±0,03	I,000±0,03
3,20 ±0,03	I,237±0,02	I,257±0,03	I,273±0,03	I,272±0,03	I,212±0,03	I,181±0,03	I,116±0,03	I,107±0,03	I,105±0,03	I,041±0,03	I,000±0,03
3,80 ±0,03	I,199±0,05	I,301±0,06	I,09±0,06	I,212±0,07	I,098±0,05	I,006±0,05	I,118±0,05	I,062±0,05	0,966±0,05	I,014±0,05	I,000±0,05
4,00 ±0,025	I,249±0,02	I,232±0,05	I,231±0,05	I,177±0,05	I,185±0,05	I,122±0,05	I,151±0,04	I,039±0,04	0,988±0,04	0,942±0,05	I,000±0,05

	$A \pm \Delta A$	W(11,5°)	W(18°)	W(30°)	W(45°)	W(60°)	W(75°)	W(85°)
0,950±0,03	I,539±0,03	I,465±0,04	I,493±0,04	I,352±0,04	I,252±0,04	I,157±0,03	I,022±0,03	I,000±0,03
I,25 ±0,05	I,471±0,01	I,448±0,03	I,444±0,03	I,363±0,03	I,185±0,03	I,090±0,03	I,031±0,03	I,000±0,03
I,35 ±0,04	I,393±0,01	I,366±0,02	I,307±0,02	I,198±0,02	I,096±0,02	I,008±0,02	I,008±0,02	I,000±0,02
I,45 ±0,04	I,418±0,02	I,365±0,03	I,281±0,03	I,181±0,02	I,036±0,02	0,978±0,02	0,978±0,02	I,000±0,02
I,55 ±0,04	I,539±0,01	I,499±0,03	I,443±0,03	I,331±0,03	I,156±0,02	0,994±0,02	0,994±0,02	I,000±0,02
I,65 ±0,03	I,442±0,01	I,451±0,03	I,336±0,03	I,263±0,03	I,150±0,03	I,019±0,02	I,019±0,02	I,000±0,02
I,75 ±0,03	I,251±0,01	I,221±0,02	I,189±0,02	I,143±0,02	I,069±0,02	0,984±0,02	0,984±0,02	I,000±0,02
I,85 ±0,03	I,248±0,01	I,269±0,03	I,233±0,03	I,210±0,03	I,151±0,03	I,055±0,03	I,055±0,03	I,000±0,02
I,95 ±0,04	I,234±0,02	I,173±0,02	I,192±0,02	I,157±0,02	I,069±0,02	0,971±0,02	0,971±0,02	I,000±0,02
2,40 ±0,025	I,271±0,02	I,265±0,04	I,228±0,04	I,152±0,03	I,157±0,03	I,008±0,03	I,008±0,03	I,000±0,03
2,60 ±0,025	I,269±0,01	I,217±0,02	I,181±0,02	I,139±0,02	I,069±0,02	0,983±0,02	0,983±0,02	I,000±0,02
3,00 ±0,03	I,251±0,01	I,251±0,02	I,201±0,02	I,139±0,02	I,050±0,02	I,033±0,02	I,011±0,02	I,000±0,02
3,40 ±0,03	I,220±0,01	I,218±0,02	I,189±0,02	I,154±0,02	I,098±0,02	I,043±0,02	I,011±0,02	I,000±0,02

VARIATION IN THE RATIO OF FISSION FRAGMENT YIELDS FROM DELAYED NEUTRON PRECURSORS IN PLUTONIUM-239 AND URANIUM-233 FISSION AT 18–21 MeV

B.P. Maksyutenko, R. Ramazanov, M.Z. Tarasko

The authors determine the relative yields of delayed neutrons in plutonium-239 and uranium-233 fission by 18–21 MeV neutrons. The research was carried out in a Van de Graaff accelerator, using the $T(d,n)^4He$ reaction with a target thickness of about 1.6 mg/cm^2.

Compared with the results obtained by the authors in earlier measurements with a thicker target (~ 20 mg/cm^2) [1], the structure of the yield ratio was more clearly pronounced, as was expected.

The authors discuss the possible reasons for this effect from the standpoint of the charge distribution in fission, with fission-inducing neutrons of different energies.

Table 1

Relative yields of delayed neutrons from plutonium-239

$T_{\frac{1}{2}}$ sec	Precursor	Relative yields		
		E_n = 18.0 MeV	E_n = 18.2 MeV	E_n = 18.5 MeV
55,65	Br^{87}	I	I	I
24,40	J^{137} (Cs^{141})	2,89±0,10	5,101±0,051	1,669±0,082
15,85	Br^{88}	1,88±0,15	4,219±0,069	3,141±0,061
11,30	Sb^{134}	1,85±0,18	1,79 ±0,12	~ 4.10^{-2}
6,05	J^{138}, Rb^{93}	0,95±0,47	3,22 ±0,18	~ 0,1
4,45	Br^{89} (Rb^{92})	3,63±0,30	~ 0,6	2,18±0,20
2,67	Rb^{94}	4,19±0,17	~ 0,2	7,27±0,19
2,02	As^{85}, J^{139} (Cs^{142}, Kr^{92})	3,04±0,76	~ 0,6	~ 0,4
1,70	Cs^{143} (Xe^{141})	2,44±1,01	2,36±0,69	~ 3.10^{-2}
1,60	Br^{90}, Sb^{135}	2,26±1,23	4,34±0,61	~ 10^{-2}
1,30	Kr^{93} (Xe^{142})	~ 2	50,46±0,26	~ 10^{-4}
		E_n=18,8 MeV	E_n=19,0 MeV	E_n=19,5 MeV
55,65	Br^{87}	I	I	I
24,40	J^{137} (Cs^{141})	3,241±0,024	5,892±0,038	5,153±0,027
15,85	Br^{88}	1,402±0,046	0,519±0,010	1,349±0,064,
11,30	Sb^{134}	1,039±0,064	1,18 ±0,12	0,71 ±0,11
6,05	J^{138}, Rb^{93}	1,17 ±0,11	2,61 ±0,15	1,39 ±0,14
4,45	Br^{89} (Rb^{92})	1,55 ±0,1	1,93 ±0,22	2,14 ±0,15

$T_{\frac{1}{2}}$ sec	Precursor	Relative yields		
		E_n = 18.8 MeV	E_n = 19.0 MeV	E_n = 19.5 MeV
2,67	Rb^{94}	4,98±0,II	4,29±0,25	4,54±0,I7
2,02	As^{85}, J^{I39} (Cs^{I42}, Kr^{92})	5,6I±0,I5	6,56±0,28	4,33±0,24
I,70	Cs^{I43} (Xe^{I4I})	3,77±0,2I	5,65±0,38	2,93±0,33
I,60	Br^{90}, Sb^{I35}	3,03±0,29	4,95±0,46	2,35±0,46
I,30	Kr^{93} (Xe^{I42})	I,I7±0,63	2,42±0,96	~ 0,9
		=20,0 MeV	=20,5 MeV	=2I,0 MeV
55,65	Br^{87}	I	I	I
24,40	J^{I37} (Cs^{I4I})	6,444±0,026	4,733±0,039	5,805±0,03I
I5,85	Br^{88}	0,5I8±0,036	I,666±0,085	I,086±0,089
II,30	Sb^{I34}	0,552±0,042	0,9I± 0,I3	0,69 ±0,I3
6,05	J^{I38}, Rb^{93}	3,I8 ±0,II	0,97 ±0,24	I,05 ±0,20
4,45	Br^{89} (Rb^{92})	3,77 ±0,I3	I,I9 ±0,26	2,I9 ±0,I7
2,67	Rb^{94}	2,I3 ±0,27	2,9I ±0,29	6,60 ±0,I7
2,02	As^{85}, J^{I39} (Cs^{I49}, Kr^{92})	2,I5 ±0,37	5,7I ±0,30	3,58 ±0,33
I,70	Cs^{I43} (Xe^{I4I})	2,58 ±0,40	6,I4 ±0,33	I,03 ±0,7I
I,60	Br^{90}, Sb^{I35}	2,8I ±0,46	5,65± 0,4I	~ 0,6
I,30	Kr^{93} (Xe^{I42})	3,77 ±0,57	2,54 ±0,85	~ 0,04

Table 2

Relative yields of delayed neutrons from uranium-233

$T_{\frac{1}{2}}$ sec	Precursor	Relative yields		
		E_n = 18.0 MeV	E_n = 18.2 MeV	E_n = 18.5 MeV
55,65	Br^{87}	I	I	I
24,40	J^{I37} (Cs^{I4I})	I,4I2±0,037	~ 3.10^{-3}	I,78I±0,028
I5,85	Br^{88}	0,385±0,087	2,4I±0,06	0,II6±0,043
II,30	Sb^{I34}	I,I48±0,06I	~ 3.10^{-2}	0,7I8±0,02I
6,05	J^{I38}, Rb^{93}	0,846±0,04I	~ 5.10^{-3}	2,535±0,066
4,45	Br^{89} (Rb^{92})	I,03 ±0,I5	~ 5.10^{-2}	0,847±0,045
2,67	Rb^{94}	I,99 ±0,I8	2,65±0,26	0,809±0,077
2,02	As^{85}, J^{I39} (Cs^{I42}, Kr^{92})	I,57 ±0,28	4,93±0,49	I,57 ±0,25
I,70	Cs^{I43} (Xe^{I4I})	I,I2 ±0,39	2,39±0,45	I,7I ±0,28
I,60	Br^{90}, Sb^{I35}	0,97 ±0,I6	I,5I±0,67	I,59 ±0,34
I,30	Kr^{93} (Xe^{I42})	0,58 ±0,28	~0,2	0,87 ±0,2I

$T_{\frac{1}{2}}$ sec	Precursor	Relative yields		
		E_n = 18.8 MeV	E_n = 19.0 MeV	E_n = 19.5 MeV
55,65	Br^{87}	I	I	I
24,40	$J^{137}(Cs^{141})$	I,0I2±0,038	I,223±0,044	0,960±0,029
I5,85	Br^{88}	I,8I4±0,036	I,373±0,05I	2,243±0,024
II,30	Sb^{134}	0,4I9±0,027	0,673±0,086	0,249±0,084
6,05	J^{138}, Rb^{93}	0,234±0,097	0,6I ±0,I3	~ 0,I
4,45	$Br^{89}(Rb^{92})$	0,7I6±0,049	0,5I ±0,I6	0,632±0,084
2,67	Rb^{94}	2,97 ±0,I3	I,34 ±0,I3	2,688±0,052
2,02	As^{85}, $J^{139}(Cs^{142}, Kr^{92})$	2,99 ±0,I8	3,055±0,096	I,596±0,079
I,70	$Cs^{143}(Xe^{141})$	2,056±0,250	2,86 ±0,II	0,932±0,036
I,60	Br^{90}, Sb^{135}	I,67 ±0,33	2,38 ±0,I2	0,769±0,04I
I,30	$Kr^{93}(Xe^{142})$	0,63 ±0,24	0,66 ±0,26	0,42 ±0,I9
		E_n=20,0 MeV	E_n=20,5 MeV	E_n=2I,0 MeV
55,65	Br^{87}	I	I	I
24,40	$J^{137}(Cs^{141})$	2,286±0,024	2,0I3±0,0I5	2,052±0,0I5
I5,85	Br^{88}	0,323±0,0I7	0,884±0,028	0,79I±0,029
II,30	Sb^{134}	I,092±0,034	0,78I±0,035	0,78I±0,035
6,05	J^{138}, Rb^{93}	I,357±0,057	0,776±0,066	0,78I±0,066
4,45	$Br^{89}(Rb^{92})$	0,746±0,03I	I,II5±0,069	0,927±0,075
2,67	Rb^{94}	I,58 ±0,II	I,6II±0,097	2,229±0,083
2,02	As^{85}, $J^{139}(Cs^{142}, Kr^{92})$	2,99 ±0,I2	I,32 ±0,I5	2,69 ±0,0I
I,70	$Cs^{143}(Xe^{141})$	2,80 ±0,I3	I,I0 ±0,I9	2,24 ±0,I4
I,60	Br^{90}, Sb^{135}	2,44 ±0,I8	I,02 ±0,24	I,99 ±0,I7
I,30	$Kr^{93}(Xe^{142})$	0,99 ±0,I2	0,87 ±0,36	I,I3 ±0,3I

I.V. Kurchatov Institute of Atomic Energy

MEASUREMENTS OF FISSION CROSS SECTIONS AND ANISOTROPY IN URANIUM-232 FISSION BY 0.1-1.5 MeV NEUTRONS

P.E. Vorotnikov, S.M. Dubrovina, G.A. Otroshchenko, V.A. Shigin*/
A.V. Davydov, E.S. Palshin**/

The authors made these measurements in an electrostatic accelerator. The fission fragments were monitored by glass detectors at angles of 0°, 30°, 60° and 90° to the neutron flux. The Table of cross-sections gives only the relative error; the error in conversion to absolute values is about 15%.

Table I

Fission cross-section of uranium-232

E_n, keV	ΔE_n, keV	σ_f, barn	$\Delta \sigma_f$, barn
125	10	2,72	0,03
180	10	2,53	0,03
220	10	2,35	0,04
265	17	2,33	0,04
280	10	2,16	0,06
390	15	2,20	0,04
420	15	2,11	0,03
530	15	2,02	0,04
625	15	2,11	0,03
680	15	2,19	0,04
730	15	2,16	0,03
825	15	2,19	0,04
880	15	2,19	0,03
920	15	2,18	0,03
1020	15	2,26	0,05
1030	15	2,19	0,06
1120	15	2,16	0,03
1220	15	2,22	0,04
1230	15	2,25	0,06
1320	15	2,20	0,04
1400	15	2,15	0,04
1480	15	2,27	0,09

*/ I.V. Kurchatov Institute of Atomic Energy.

**/ Institute of Geochemistry and Analytical Chemistry.

Table II

Fission anisotropy of uranium-232

E_n, keV	ΔE_n, keV	A	Δ A
I25	I0	I,I5	0,04
I80	I0	I,I8	0,04
220	I7	I,I6	0,04
230	I0	I,23	0,I0
265	I7	I,I9	0,05
280	I0	I,I8	0,06
380	I5	I,27	0,06
390	I5	I,22	0,05
420	I5	I,I4	0,04
480	I5	I,02	0,04
520	I5	I,07	0,04
530	I5	I,06	0,04
580	I5	0,99	0,04
625	I5	0,96	0,04
680	I5	0,97	0,03
690	I5	0,97	0,04
730	I5	0,99	0,03
780	I5	I,I8	0,06
785	I5	I,I0	0,05
825	I5	I,06	0,03
880	I5	I,09	0,04
920	I5	0,97	0,03
980	I5	I,03	0,03
I020	I5	I,06	0,04
I030	I5	I,05	0,05
II20	I5	I,09	0,03
I220	I5	I,I5	0,04
I230	I5	I,I4	0,05
I320	I5	I,I5	0,04
I330	I5	I,I8	0,04
I400	I5	I,I4	0,04
I480	I5	I,I5	0,09
5000	I5	I,I4	0,04

AVERAGE NUMBER OF PROMPT NEUTRONS PER FISSION IN URANIUM-235, PLUTONIUM-239 AND PLUTONIUM-240 FISSION BY FAST NEUTRONS

M.V. Savin, Yu.A. Khokhlov, Yu.S. Zamyatnin, I.N. Paramonova

The authors report measurements of the average number of neutrons per fission ($\bar{\nu}$) in uranium-235, plutonium-239 and plutonium-240 fission by 0.7-5 MeV neutrons. The measuring technique is described in detail in Ref. [1]. The primary neutrons were produced in the lead target of a linear accelerator bombarded by electron pulses lasting 30 nsec. The neutrons and fission gamma rays were recorded by a 400-litre liquid scintillation detector. The primary neutrons were selected by the time-of-flight method with a time resolution of 1 nsec/m, and the fission events were monitored from the prompt fission gamma rays.

The weights of the samples used for the measurements were 30.7 g of uranium-235 (90% enriched), 24.21 g of plutonium-239 (98% enriched) and 10 g of plutonium-240 (81.47% ^{240}Pu, 9.17% ^{239}Pu, and 9.36% ^{241}Pu). The uranium-235 and plutonium-239 samples consisted of sets of metal discs 15 mm in diameter and 1 mm thick. The plutonium-240 sample was in dioxide form and was contained in a plastic glass vessel.

The background of neutrons scattered elastically and inelastically on the specimens studied - which at E_n = 0.7-5 MeV slightly exceeded the random coincidence background - was taken into account in measurements with a lead sample.

The $\bar{\nu}$ values for uranium-235, plutonium-239 and plutonium-240 were derived by comparison with $\bar{\nu}$ = 3.772 $\pm$ 0.000 for spontaneous fission of californium-252.

The following corrections were introduced into the $\bar{\nu}$ values:

1. A correction for the angular correlation fission neutron/incident neutron, due to the angular anisotropy of the fission fragments;
2. A correction for fluctuations in detector efficiency due to changes in the fission neutron energy spectrum with increasing $\bar{\nu}$, and for the difference between the ^{252}Cf neutron spectrum and the fission neutron spectra of the isotopes studied;
3. A correction for isotopic impurities in the samples.

The Table shows the mean square absolute measurement errors. The relative error in measuring $\bar{\nu}$ is 0.8% for uranium-235 over the energy range E_n = 0.6-5 MeV, and 1% for plutonium-239 over the range E_n = 0.7-4.5 MeV.

REFERENCE

[1] SAVIN, M.V., KHOKHLOV, Yu.A., ILYIN, Yu.I., SHEIN, Yu.V. PTE 6 (1969).

Table 1

$\bar{\nu}$ for ^{240}Pu, ^{239}Pu, ^{235}U

^{240}Pu		^{239}Pu		^{235}U	
E_n MeV	$\bar{\nu}$	E_n MeV	$\bar{\nu}$	E_n MeV	$\bar{\nu}$
I,08	3,I38±0,I56	0,89	3,026±0,070	0,65	2,432±0,039
I,I5	3,22I±0,I6I	0,96	3,005±0,060	0,68	2,447±0,039
I,23	3,0I8±0,I20	0,99	3,0II±0,060	0,7I	2,472±0,039
I,3I	3,038±0,I06	I,03	3,049±0,046	0,73	2,473±0,039
I,39	3,037±0,I06	I,07	3,009±0,046	0,79	2,478±0,039
I,46	3,05I±0,II2	I,I0	3,053±0,046	0,82	2,49I±0,040
I,54	3,I9I±0,I02	I,I4	3,089±0,047	0,87	2,474±0,039
I,62	3,260±0,097	I,I7	3,066±0,046	0,9I	2,499±0,040
I,7I	3,I70±0,095	I,22	3,06I±0,046	0,97	2,484±0,039
I,8I	3,264±0,09I	I,26	2,984±0,045	I,0I	2,49I±0,039
I,92	3,238±0,090	I,30	3,02I±0,045	I,06	2,539±0,038
2,02	3,I75±0,I04	I,34	3,I29±0,047	I,I5	2,575±0,038
2,I5	3,I5I±0,I04	I,39	3,II8±0,047	I,25	2,578±0,038
2,29	3,280±0,II4	I,49	3,I38±0,047	I,35	2,6I3±0,039
2,39	3,262±0,II4	I,54	3,I65±0,047	I,4I	2,6I8±0,039
2,50	3,435±0,I27	I,60	3,I35±0,045	I,48	2,636±0,039
2,62	3,367±0,I34	I,66	3,I00±0,045	I,63	2,64I±0,039
2,74	3,327±0,I33	I,72	3,I42±0,047	I,80	2,64I±0,039
2,88	3,450±0,I38	I,78	3,203±0,048	I,97	2,645±0,039
3,02	3,423±0,I43	I,85	3,2I7±0,048	2,05	2,66I±0,040
3,I8	3,484±0,I56	I,9I	3,220±0,048	2,I8	2,700±0,033
3,53	3,50I±0,I57	I,97	3,243±0,048	2,26	2,7I3±0,035
3,73	3,406±0,I70	2,05	3,I63±0,047	2,39	2,748±0,035
3,94	3,507±0,200	2,I4	3,I76±0,047	2,55	2,7II±0,035
		2,23	3,230±0,048	2,68	2,763±0,033
		2,36	3,227±0,048	2,85	2,8I2±0,034
		2,49	3,3I0±0,049	2,94	2,806±0,034
		2,59	3,304±0,049	3,06	2,800±0,034
		2,67	3,338±0,057		
		2,79	3,320±0,056	3,28	2,833±0,043
		3,0I	3,364±0,057	3,7I	2,87I±0,043
		3,2I	3,4I5±0,06I	4,23	2,903±0,044
		3,34	3,395±0,06I	4,57	2,937±0,058
		3,52	3,387±0,06I	4,90	3,032±0,06I
		3,72	3,379±0,067	5,32	3,095±0,072
		3,94	3,439±0,075	5,60	3,II0±0,082
		4,05	3,579±0,078	5,94	3,234±0,I06
		4,23	3,558±0,089	6,60	3,373±0,III
		4,35	3,55I±0,089		
		4,49	3,66I±0,09I		
		4,70	3,684±0,II0		

THERMALIZATION OF NEUTRONS IN H_2O AT 318°K AND 77°K

S.N. Ishmaev, I.P. Sadikov and A.A. Chernyshov

Experiments were carried out to study the thermalization of neutrons as a function of time in water (T = 318°K) and in ice (T = 77°K) by measuring the time dependence of neutron fluxes with several fixed energies. For this purpose a crystal spectrometer coupled to a pulsed fast-neutron source was used. The authors describe their method of measurement and discuss its advantages and limitations as compared with the phased chopper method used earlier.

It is demonstrated in the paper that the channel used to remove the neutron beam from the water system greatly distorts the results of the measurements. The perturbations due to the channel are the main reason for discrepancies with theory observed in previous measurements of non-steady neutron spectra in water.

The experimental results obtained for water agree with the earlier theoretical calculations based on Nelkin's model for water. The measurements in water at two temperatures show that the establishment of an equilibrium neutron spectrum with time depends to a considerable extent on the temperature of the medium. Analysis of the experimental results suggests that both in water and ice (at T = 77°K) the dispersion operator for the non-stationary Boltzmann equation has a zero and a first discrete eigenvalue.

The following times were obtained for thermalization of neutrons in H_2O: 5.8 ± 0.6 μsec (at T = 318°K) and 55.5 ± 1.5 μsec (at T = 77°K).

Joint Institute for Nuclear Research

MEASUREMENT OF THE RADIATIVE CAPTURE TO FISSION CROSS-SECTION RATIO (α) FOR PLUTONIUM-239 IN THE NEUTRON ENERGY RANGE 0.1-30 keV

M.A. Kurov, Yu.V. Ryabov, So Don Sik, N. Chikov, V.N. Kononov
E.D. Poletaev, Yu.S. Prokopets, Yu.Ya. Stavissky

Using the time-of-flight spectrometer of the Joint Institute for Nuclear Research (JINR), with resolving times of 15 and 220 nsec/m, the authors measured $\alpha(E)$ for plutonium-239. The experimental procedure consisted in comparing counts from an ionization fission chamber containing "thin" layers of plutonium-239 with those from a large liquid scintillation detector recording radiative capture and fission gamma rays from a "thick" sample of plutonium-239. The fission cross-sections $\sigma_f(E)$ and $\alpha(E)$ were normalized to known values of $\sigma_o\Gamma_f$ and α_i for low-energy resonances. The path of the neutron flux was measured with a "thin" boron counter.

The values of $\langle\sigma_f(E)\rangle$ obtained throughout the energy interval are systematically 5-20% higher than those recommended by James and Patrick (Harwell), while up to 2 keV $\langle\alpha(E)\rangle$ coincides with earlier published data (Dubna, 1968) within the limits of the experimental errors, and above 2 keV it is 1.5-2 times lower than the familiar data of Sowerby and Patrick (Harwell).

Table I

Mean cross-sections $\langle\sigma_f(E)\rangle$ for plutonium-239 measured with time resolutions of 15 nsec/m (1) and 220 nsec/m (2) (same data as in 70Helsinki, Vol.1,p.345)

E,KeV	$\langle\sigma_f(E)\rangle$ 15 nsec/m	220 nsec/m	$\langle\sigma_f(E)\rangle$ (Harwell)
20-29,6	2,05	I,7I	I,57
I0,I-20	2,09	2,I3	I,7I
9,I-I0,I	2,22	2,I7	2,06
8-9,I	2,32	2,26	2,25
7-8	2,55	2,35	2,I4
6-7	2,I3	2,09	2,I9
5-6	2,36	2,50	2,50
4-5	2,65	2,67	2,45
3-4	3,65	2,95	2,95
2-3	3,6I	2,9I	3,07
I-2	5,56	5,0I	3,85
0,9-I	I0,93	6,I6	
0,8-0,9	7,03	5,68	
0,7-0,8	6,57	5,34	
0,6-0,7	7,34	7,32	
0,5-0,6	I8,33	I3,6I	
0,4-0,5	I2,30	9,38	
0,3-0,4	7,30	9,34	
0,2-0,3	I7,88	I9,I5	
0,I-0,2	21,63	I8,94	

Table II

Values of α_o for resolved resonances used for calibration

Laboratory E_o, eV	Saclay	ANL	BNL	Harwell	ORNL - RPI	Nuclear Physics Laboratory (LNF)	JINR
7,83	0,85±0,09	0,98±0,10	1,04±0,09	1,0±0,1	0,85±0,02	0,84±0,04	0,87±0,07	0,85±0,02
10,97	0,38±0,08	0,22±0,10	0,32±0,08	0,36±0,08	0,27±0,05	0,24±0,03	0,27±0,04	0,35±0,08
11,91	1,75±0,25	1,86±0,35	1,86±0,20	1,59±0,20	1,56±0,10	1,52±0,10	1,38±0,21	1,54±0,16
14,36	0,51±0,14	0,66±0,16	0,82±0,20	0,67±0,13	0,55±0,02	0,58±0,04	0,67±0,10	-
14,75	1,25±0,07	1,21±0,18	1,32±0,25	1,31±0,13	1,13±0,05	1,11±0,08	1,25±0,14	
17,69	1,15±0,04	0,84±0,21	1,0±0,2	1,15±0,10	1,14±0,05	-	0,92±0,13	1,04±0,08
22,33	0,71±0,07	0,46±0,24	0,59±0,14	0,76±0,07	0,64±0,01	-	0,71±0,06	0,80±0,08
26,31	0,84±0,17	1,07±0,21	1,22±0,26	1,21±0,15	0,91±0,03	0,91±0,05	0,68±0,21	0,82±0,09
44,6	9,28±0,40	9,61±0,91	7,3±1,7	8,5±0,5	9,52±1,00	9,38±0,30	4,6±2,5	-
47,92	0,31±0,10	0,13±0,05	0,16±0,07	0,36±0,08	0,32±0,06	-	0,11±0,06	-
50,18	3,5±0,4	1,20±0,33	1,27±0,23	2,08±0,30	-	2,45±0,10	1,51±0,43	-
52,8	5,25±0,20	4,40±0,66	4,6±1,2	4,99±0,49	-	5,22±0,20	4,1±0,9	-

Table III

α	Calibration error
0,2	35%
0,5	14,8%
1	7,4%
1,5	4,9%

Table IV

Averaged value of $<\alpha>$ for plutonium-239 obtained in a series of measurements with time resolutions of 15 nsec/m (1) and 220 nsec/m (2)

Averaging interval E, keV	$<\alpha>$(1)	$<\alpha>$(2)
I0,I-29,5	0,48±0,I0	0,36±0,08
9,I-I0,I	0,43±0,06	0,46±0,09
8-9,I	0,49±0,06	0,43±0,08
7-8	0,46±0,07	0,44±0,08
6-7	0,97±0,08	0,59±0,I0
5-6	0,90±0,05	0,65±0,09
4-5	0,95±0,08	0,7I±0,08
3-4	0,67±0,08	0,77±0,II
2-3	0,89±0,I4	0,83±0,I4
I-2	0,65±0,I4	0,78±0,I3
0,9-I	0,48±0,II	0,65±0,I5
0,8-0,9	0,68±0,I4	0,63±0,I4
0,7-0,8	I,03±0,07	0,70±0,I6
0,6-0,7	0,75±0,I3	0,92±0,2I
0,6-0,6	0,68±0,I0	0,70±0,I0
0,4-0,5	0,48±0,I6	0,60±0,I2
0,3-0,4	I,7I±0,28	0,82±0,23
0,2-0,3	I,3I±0,23	0,72±0,I6
0,I-0,2	0,7I±0,07	0,73±0,05

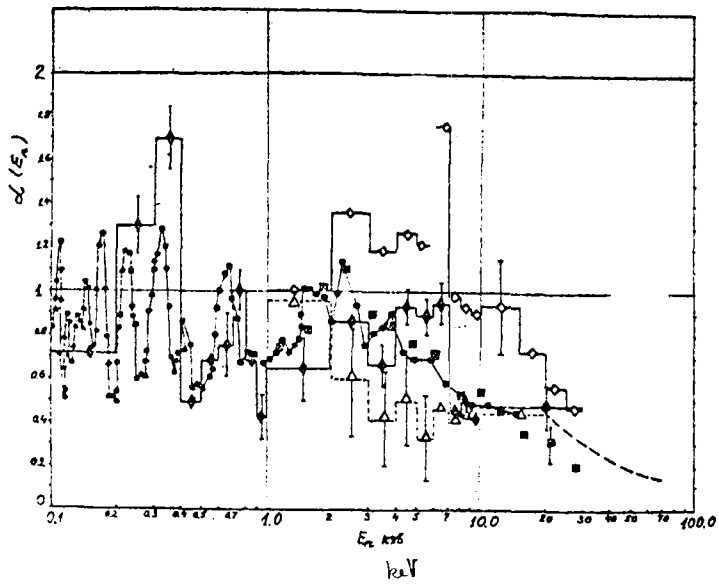

Fig. 1. Measurement of α between 0.1 and 100 keV

—⊙— - This paper;energy resolution 220 nsec/m.

—◈— - This paper;energy resolution 15 nsec/m (specimen 0.7 x 10^{21} nuclei/cm^2).

⊠ - Data taken from Gwin and co-workers.

– –△– – - Data obtained at Dubna, 1968.

—◇— - Data (we give the mean result obtained by Sowerby and co-workers for several series of measurements).

– – – – – - BNL report 325, Supplement N2.

RELATIVE MEASUREMENTS OF $\bar{\nu}$ IN URANIUM-235 AND PLUTONIUM-239 FISSION BY RESONANCE NEUTRONS

Yu.V. Ryabov, So Don Sik, N. Chikov, N. Yaneva

Using the time-of-flight spectrometer belonging to the Neutron Physics Laboratory of the Joint Institute for Nuclear Research, the authors measured the average number of prompt neutrons per fission in certain resonances of uranium-235 and plutonium-239. For their measurements they used a large liquid scintillation detector containing cadmium propionate to monitor the fast fission neutrons. The moment of fission was recorded from the prompt gamma rays.

The results obtained indicate that $\bar{\nu}$ is a function of the compound nucleus spin level g factor. Interpretation of the results in accordance with the channel theory makes it possible to evaluate the difference in the heights of the effective barriers during fission via the 4^- and 3^- states in the case of uranium-235 ($\Delta E_\delta = 0.33 \pm 0.16$ MeV), and the 1^+ and 0^+ states in the case of plutonium-239 ($\Delta E_\delta = 0.93 \pm 0.27$ MeV).

Table I

Correlation coefficients $r(a_i b_i)$ for uranium-235 and plutonium-239

	$r(a_i b_i)$	^{235}U	^{239}Pu
$\frac{\bar{\nu}_i}{\langle\bar{\nu}_i\rangle}$	Relative yield of fragments with symmetric mass, M_C/M_A	0.42 ± 0.16	-0.59 ± 0.14
$\frac{\bar{\nu}_i}{\langle\bar{\nu}_i\rangle}$	Spin level g factor	$\frac{0.34\pm0.18}{0.50\pm0.17 \text{(up to 20 eV)}}$	0.84 ± 0.08
$\bar{\nu}_i/\langle\bar{\nu}_i\rangle$	Γ_{fi}	-0.46 ± 0.16	-0.56 ± 0.15
$\bar{\nu}_i/\langle\bar{\nu}_i\rangle$	Γ^o_{ni}	-0.11 ± 0.20	-0.02 ± 0.22
$\bar{\nu}_i/\langle\bar{\nu}_i\rangle$	$(\sigma_o \Gamma_f)_i$	-0.07 ± 0.20	0.04 ± 0.22

Table II

Mean values of $\bar{\nu}_i/\langle\bar{\nu}_i\rangle$ and Γ_f for two groups of levels of uranium-235 and plutonium-239

Separation method	^{235}U		^{239}Pu	
	Group 1	Group 2	Group 1	Group 2
Sum of two Gaussian distributions (least squares)	1.006±0.008	0.984±0.006	1.013±0.007	0.974±0.010
From the spin g factor	1.005±0.002	0.990±0.002	1.014±0.003	0.977±0.005
From the relative yield of fragments with symmetric mass (M_C/M_A)	1.007±0.002	0.990±0.002	1.007±0.003	0.973±0.008
From the value $\bar{\nu}_i/\langle\bar{\nu}_i\rangle$	$\langle\Gamma_f\rangle$	^{235}U	$\langle\Gamma_f\rangle$	^{239}Pu
	31±3	70±6	50±8	432±85

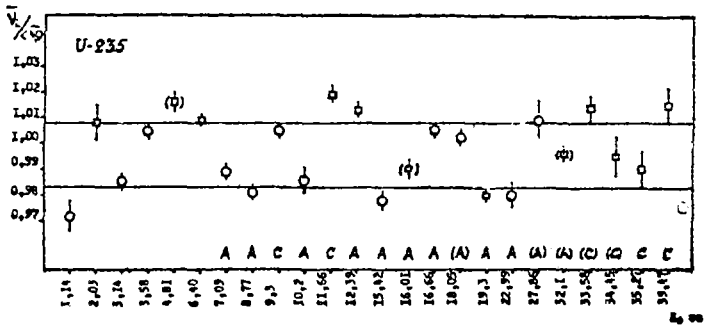

Fig. 1 $\bar{\nu}_i/\langle\bar{\nu}_i\rangle$ for ^{235}U
A,C - mainly asymmetric and symmetric fission (Los Alamos)
□ - $J = 4^-$) determination of spin from multiplicity of
0 - $J = 3^-$) γ rays (Saclay)

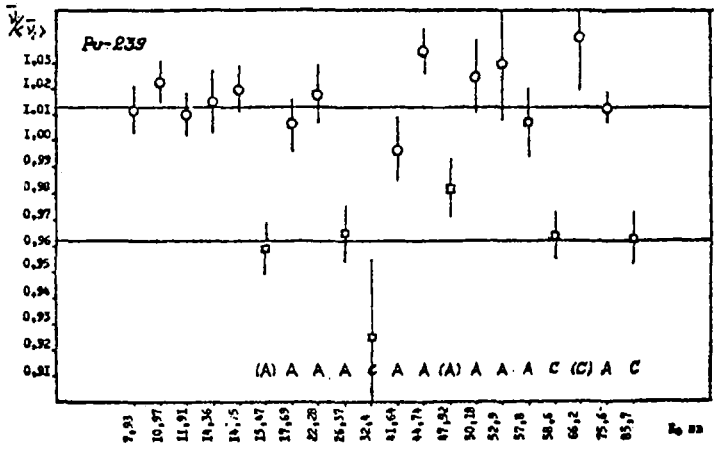

Fig. 2 $\bar{\nu}_i/\langle\nu_i\rangle$ for ^{239}Pu
A,C - mainly asymmetric and symmetric fission (Los Alamos)
□ - $J = 0^+$) determination of spin from measurement of
0 - $J = 1^+$) resonance neutron scattering (Harwell)

Radium Institute of the USSR Academy of Sciences

MEASUREMENT OF ^{238}U FISSION CROSS-SECTIONS FOR 2.5 MeV NEUTRONS WITH NEUTRON FLUX DETERMINATION BY THE ASSOCIATED PARTICLE METHOD

I.M. Kuks, V.I. Matvienko, Yu.A. Nemilov, K.A. Petrzhak, Yu.A. Selitsky and V.B. Funshtein

(Submitted to Atomnaja Energija)

The ^{238}U fission cross-sections available in the literature for neutrons in the region of the first plateau were derived either by a relative method or by determining the neutron flux from recoil protons. The most direct method of monitoring the neutron flux - from the associated charged particles - has been applied to measurements of σ_f in the past only for E_n = 14 MeV from the reaction $T(d,n)^4He$. In this work the authors measured the fission cross-section of ^{238}U for 2.5 MeV neutrons from the reaction $D(d,n)^3He$. The neutron flux was determined from the accompanying alpha particles, which were separated from the protons and tritons resulting from the parallel D(d,p)T reaction by a gas proportional counter. The fission cross-section derived in this way is 0.55 ± 0.02 barns, which coincides with the latest value recommended in the literature [1].

REFERENCE

[1] HART, I.W., Authority Health and Safety Branch, UKEAEA, R., 169, (1969).

THE SPONTANEOUS FISSION PERIOD OF CALIFORNIUM-252

B.M. Aleksandrov, M.A. Bak, V.G. Bogdanov,
S.S. Bugorkov, L.V. Drapchinsky, Z.I. Solovyeva, A.V. Sorokina

(Submitted to Atomnaja Energija)

In small solid angle geometry, using a semi-conductor detector and thick-layer photoemulsions, the authors measured the ratio between the number of alpha decays and the number of spontaneous fissions in a single californium-252 sample. Comparison of the results obtained with those available in the literature made it possible to calculate the weighted mean of this ratio. The resultant data are shown in the Table. They do not include the results obtained by the ionization chamber and thick-plate method in near-2π geometry since, as shown in the paper, absorption of fission fragments in the layer of fissionable material gives a ratio that is too high.

Table

Recording method	Ratio of alpha decays to spontaneous fissions for ^{252}Cf	Error	Author
Semi-conductor detector	31.5	$\pm$ 0.3	Present paper
Photoemulsion	31.1	$\pm$ 0.5	Present paper
Semi-conductor detector	31.3	$\pm$ 0.2	[1]
Mean weighted value	31.34	$\pm$ 0.08	

Applying this mean weighted ratio of the number of alpha decays to the number of spontaneous fissions and the most reliable value of the total decay constant for californium-252 ($\lambda = (7.212 \pm 0.017) \times 10^{-4}$ d^{-1}, from Ref. [2]) we arrive at a constant for spontaneous fission of ^{252}Cf:

$\lambda_{s.f.} = (2.227 \pm 0.011) \times 10^{-5}$ d^{-1}, which gives the value $T_{s.f.} = 85.2 \pm 0.4$y as the spontaneous fission half-life.

REFERENCES

[1] METTA, D., DIAMOND, H., BARNES, K.F., MILSTED, J., GRAY Jr. J., HENDERSON, D.J. and STEVENS, C.M., J. Inorg. Nucl. 27, Chem. No. 1, (1965) 33.

[2] DE-VOLPI, A. and PORGES, K.G., Inorg. Nucl. Chem. Letters 5, No. 2, (1969) 111.

Institute of Physics, Ukrainian Academy of Sciences

TOTAL CROSS-SECTIONS FOR SCATTERING OF SLOW NEUTRONS IN COPPER, GERMANIUM AND NATURAL RHENIUM ISOTOPES

V.V. Koloty, V.P. Vertebny

The authors determined cross-sections for neutron scattering by ^{63}Cu and ^{65}Cu, ^{70}Ge, ^{72}Ge, ^{73}Ge and ^{74}Ge, and natural mixtures of copper, germanium and rhenium isotopes. The measurements were carried out in 4π geometry on the VVR-M reactor belonging to the Institute of Physics, with resolving times of 6 and 12 μsec/m, using 0.015–1 eV neutrons. Table 1 shows the scattering cross-sections for v = 2200 m/sec.

The measurements were carried out with respect to vanadium, the scattering cross-section of which was taken as 5.1 barns. The copper samples were metal foils and the germanium isotope samples were in the form of the oxide GeO_2; the natural germanium took the form of a metal powder, and likewise the rhenium sample.

Using the cross-section data thus obtained for neutron scattering by germanium isotopes together with the data available in the literature on the resonance parameters of the levels of these isotopes, we determined the parameters of the negative levels of even-even germanium isotopes:

Ge^{70}: $E_0 = (60 \pm 30)$ eV, $\Gamma_n^0 = (19 \pm 9)$ meV;
Ge^{72}: $E_0 = (330 \pm 100)$ eV, $\Gamma_n^0 = (160 \pm 50)$ meV;
Ge^{74}: $E_0 = (1018 \pm 300)$ eV; $\Gamma_n^0 = (910 \pm 250)$ meV.

Table

Nucleus	Enrichment of sample in basic isotope	Scattering cross-section (barn)
Cu^{63}	69,1%	4,8±0,4
Cu^{65}	96,4%	11,4±0,4
Cu	-	6,9±0,3
Ge^{70}	90,0%	8,8±0,8
Ge^{72}	90,1%	7,5±0,7
Ge^{73}	71,0%	1,0±0,9
Ge^{74}	92,7%	6,1±0,4
Ge	-	7,5±0,2
Re	-	11,3±0,5

NEUTRON RESONANCES OF CAESIUM-136 AND CAESIUM-138

V.P. Vertebny, P.N. Vorona, A.I. Kalchenko, M.V. Pasechnik,
Zh.I. Pisanko, V.A. Pshenichny, V.K. Rudishin

To study the level density of nuclei located at the edge of the isotope stability valley, the authors measured the transmission of neutrons by samples enriched in ^{136}Cs (24.3%) and ^{138}Cs (12.9%), using the VVR-M reactor belonging to the Institute of Physics for the purpose. The measurements were made by the time-of-flight method over the neutron energy range 0.01-5000 eV; the maximum resolution was 50nsec/m. The data on the energy levels and resonance parameters are shown in the table below. In ^{138}Cs no levels were detected over the energy range measured. The mean distance between ^{136}Cs levels, $\bar{D}$, is 58 ± 12 eV; for ^{138}Cs it can only be assumed that $\bar{D} \gtrsim 200$ eV.

Table I

E_o eV	Γ_n^o, meV	Source
66,3±0,5	6,1±3,1	136
135,7±1,25	54,1±10,7	136
181,0±1,8	0,32±0,32	136
187 ± 2	0,31±0,31	136
231 ± 3	5,3 ± 5,3	136
274 ± 4	19±19	136
533 ± 10	35±35	136
633 ± 12	58±58	136
876 ± 20	47±47	136

RESONANCES OF THE ISOTOPES EUROPIUM-151 AND EUROPIUM-153

V.P. Vertebny, P.N. Vorona, A.I. Kalchenko, V.V. Koloty,
M.V. Pasechnik, Zh.I. Pisanko, V.A. Pshenichny
and V.K. Rudishin

Using the VVR-M reactor at the Institute of Physics and applying the time-of-flight method, the authors measured the transmission of neutrons by samples of ^{151}Eu and ^{153}Eu over the energy range 0.1-1000 eV with resolving times of 55 nsec/m and 200 nsec/m. The ^{151}Eu sample was 98.8% enriched, the ^{153}Eu sample 99.3%; the thickness of the ^{151}Eu and ^{153}Eu samples in terms of the principal isotopes was 14.99×10^{20} nuclei/cm^2 and 17.52×10^{20} nuclei/cm^2, respectively. Tables I and II show the respective level energies for ^{151}Eu and ^{153}Eu.

Table I

Neutron resonances of the isotope ^{151}Eu

E_o, eV	E_o, eV
0,320	I7,82 ± 0,I2
0,459 ± 0,002	I9,22 ± 0,I3
I,063 ± 0,007	I9,9* ± 0,I3
I,8I5 ± 0,007	2I,87 ± 0,I6
2,523 ± 0,025	22,37 ± 0,I7
2,740 ± 0,030	22,88 ± 0,I7
3,383 ± 0,0I0	24,73 ± 0,20
3,735 ± 0,0I2	26,80 ± 0,2I
4,804 ± 0,0I7	27,60* ± 0,I0
5,408 ± 0,020	29,4I ± 0,26
5,968 ± 0,023	30,45 ± 0,27
6,038 ± 0,024	3I,83 ± 0,28
7,090 ± 0,0I5	33,6I ± 0,3I
7,289 ± 0,032	35,22 ± 0,33
7,448 ± 0,032	36,46 ± 0,23
7,645* ± 0,033	37,30 ± 0,36
7,886* ± 0,036	39,57 ± 0,37
8,846* ± 0,042	4I,62 ± 0,42
9,I02 ± 0,043	43,39 ± 0,45
I0,5I4 ± 0,054	47,26 ± 0,5I
II,06 ± 0,04	5I,I0 ± 0,58
II,26 ± 0,06*	52,88 ± 0,60*
I2,28 ± 0,07	58,I4 ± 0,70
I2,70 ± 0,07	63,80 ± 0,40
I3,69 ± 0,08	68,5I ± 0,90
I4,89 ± 0,08	72,3 ± I
I5,27 ± 0,I0	80,75 ± I,II
	I09,9 ± I,8

The asterisks indicate doubtful levels.

Table II

Neutron resonances of the isotope ^{153}Eu

E_o, eV	E_o, eV
0,457[X] ± 0,002	38,4I ± 0,38
I,732 ± 0,0I5	42,49 ± 0,44
2,449 ± 0,025	43,39 ± 0,45
3,3I5 ± 0,0I0	46,25[X] ± 0,50
3,963 ± 0,0I3	48,3I ± 0,53
4,787 ± 0,0I6	5I,I0 ± 0,58
6,I94 ± 0,0I2	52,88 ± 0,60
8,870 ± 0,042	54,77 ± 0,64
II,69 ± 0,07	6I,07 ± 0,7
I2,49 ± 0,07	64,2I ± 0,8
I3,30 ± 0,08	68,5I ± 0,9
I4,I0[X] ± 0,08	77,4I ± 0,9
I5,36 ± 0,09	8I,9 ± 0,9
I6,I6[X] ± 0,I0	88,2 ± 0,9
I6,79 ± 0,I0	93,7 ± I
I8,I9 ± 0,I3	I00 ± I
I8,82 ± 0,I3	I22 ± I
20,I9 ± 0,I5	I58 ± 3
22,7I ± 0,I6	I87 ± 4
23,79 ± 0,20	247 ± 5
26,37 ± 0,23	289 ± 7
28,9I ± 0,25	342 ± I0
30,I8 ± 0,26	455 ± I5
3I,54 ± 0,28	659 ± 28
34,89 ± 0,33	
36,94 ± 0,36	

The asterisks indicate doubtful levels.

FAST-NEUTRON RADIATIVE CAPTURE CROSS-SECTIONS FOR THE ISOTOPES ^{69}Ga, ^{71}Ga, ^{139}La AND ^{141}Pr

G.G. Zaikin, I.A. Korzh, M.V. Pasechnik,
and N.T. Sklyar

(Submitted to Ukrainskij fizičeskij žurnal - 1970)

Using the activation method [1,2], the authors measured radiative capture cross-sections for 0.1-5.9 MeV neutrons in the isotopes ^{69}Ga, ^{71}Ga, ^{139}La and ^{141}Pr. The energy dependence of the capture cross-section was determined relative to the fission cross-section of uranium-235. Absolute normalization of the cross-section was obtained by comparing the activities generated by irradiation with fast and thermal neutrons. The measurements were carried out in an electrostatic accelerator. The neutrons were obtained from the reactions $^{7}Li(p,n)^{7}Be$, $T(p,n)^{3}He$, and $D(d,n)^{3}He$. The activities of ^{70}Ga, ^{140}La and ^{142}Pr were determined from the beta count. The gamma rays from ^{72}Ga were monitored with a scintillation gamma spectrometer using an NaI(Tl) crystal. The measured fast-neutron radiative capture cross-sections in ^{69}Ga, ^{71}Ga, ^{139}La and ^{141}Pr are shown in Tables I-IV.

REFERENCES

[1] ZAIKIN, G.G., KORZH, I.A., SKLYAR, N.T., TOTSKY, I.A., Atom. energ. 23 (1967) 67.

[2] ZAIKIN, G.G., KORZH, I.A., PASECHNIK, M.V., SKLYAR, N.T., Programma i tezisy dokladov XX ežegodnogo soveščanija po jadernoj spektroskopii i strukture atomnogo jadra (Programme and abstracts of papers presented at the twentieth annual conference on nuclear spectroscopy and the structure of the atomic nucleus) 2 Leningrad (1970) 49.

Table I

Cross-sections for radiative capture of fast neutrons by ^{69}Ga

$E_n \pm \Delta E_n$, keV	$\sigma(n,\gamma) \pm \Delta\sigma(n,\gamma)$, mbarn
198±21	45,9±2,3
344±46	38,9±1,7
410±46	35,2±2,2
458±44	35,9±1.6
566±45	29,5±1,0
600±19	26,2±1,6
672±44	24,9±1,0

Table I continued

$E_n \pm \Delta E_n$, keV	$\sigma(n,\gamma) \pm \Delta\sigma(n,\gamma)$, mbarn
768±58	23,5±0,9
828±44	23,8±I,I
I036±45	I9,8±0,9
I2I5±66	I7,0±0,7
I234±45	I7,0±0,8
I460±70	I3,9±0,7
I7I0±77	II,6±0,6
I770±38	I0,9±0,6
I970±66	I0,4±0,4
2I40±57	8,44±0,42
2280±68	9,44±0,47
2585±70	8,5 ±0,5
3080±72	I0,5 ±0,6

Table II

Cross-sections for radiative capture of fast neutrons by ^{71}Ga

$E_n \pm \Delta E_n$, keV	$\sigma(n,\gamma) \pm \Delta\sigma(n,\gamma)$, mbarn
I98±27	4I,5±I,9
285±23	38,4±I,8
340±52	33,2±I,5
454±48	25,2±I,I
600±20	I8,5±0,8
670±46	I4,8±0,7
830±46	I4,8±0,8
I030±45	I2,I±0,6
I240±47	I0,6±0,6
I460±70	8,I±0,4
I7I0±77	6,7±0,4
I970±66	6,2±0,4
2580±68	5,2±0,4

Table III

Cross-sections for radiative capture of fast neutrons by ^{139}La

$En \pm \Delta En$, keV	$\sigma(n,\gamma) \pm \Delta\sigma(n,\gamma)$, mbarn
198±22	9,63±0,64
286±21	6,91±0,62
350±45	7,42±0,45
379±22	6,54±0,39
410±46	7,50±0,53
475±45	6,25±0,38
585±44	6,88±0,41
690±45	6,30±0,38
794±48	6,65±0,47
835±50	6,95±0,49
950±50	6,07±0,52
1120±50	7,34±0,56
1250±80	8,23±0,79
1480±70	8,46±0,42
1730±70	7,13±0,36
1980±76	5,46±0,27
2300±79	4,86±0,49
2580±68	4,1 ±0,27
2700±86	4,1 ±0,37
3100±50	3,53±0,46
5900±280	1,2 ±0,17

Table IV

Cross-sections for radiative capture of fast neutrons by ^{141}Pr

$En \pm \Delta En$, keV	$\sigma(n,\gamma) \pm \Delta\sigma(n,\gamma)$, mbarn
84±16	69,1±3,5
146±18	55,5±5,0
198±27	35,4±1,8
211±23	33,2±2,0
260±23	31,5±1,6
285±23	26,7±1,6
320±23	28,4±2,5
378±23	23,4±1,2
435±21	22,2±0,9
491±21	19,7±0,8
546±21	20,6±1,0

Table IV continued

$E_n \pm \Delta E_n$, keV	$\sigma(n,\gamma) \pm \Delta\sigma(n,\gamma)$, mbarn
590±45	I9,4±I,0
600±20	I9,5±0,8
640±4I	2I,3±I,3
670±6I	2I,2±I,0
740±4I	22,5±I,3
768±58	2I,7±I,2
845±38	25,9±I,5
925±56	22,7±I,3
945±38	24,I±I,4
II00±50	26,3±I,3
I290±50	25,3±I,4
I490±50	23,2±I,4
I730±50	20,I±I,2
I990±50	I7,I±I,0
2300±50	I4,6±0,9
2590±65	II,8±0,7
2700±50	II,6±0,8
3080±72	8,9±0,9
5900±280	2,4±0,3

POLARIZING POWER OF NUCLEI WITH MEDIUM ATOMIC WEIGHT FOR 1.5 MeV NEUTRONS

I.A. Korzh, T.A. Kostyuk, V.I. Mishchenko,
N.M. Pravdivy, I.E. Sanzhur

(Submitted to Izv. Akad. Nauk SSSR, Ser. fiz.)

The authors report experimental and theoretical results of a study of elastic scattering of polarized 1.5 MeV neutrons on Ti, Cr, Fe, Co, Ni, Cu, Zn, Zr, Nb and Mo nuclei. The polarizing power of the nuclei was determined from measurements of right-left asymmetry in scattering of partially polarized neutrons [1]. The reaction $T(p,n)^3He$ served as a source of partially polarized neutrons, and the neutrons used in the experiment emerged at an angle of 33° (in the laboratory system of co-ordinates) to the proton beam accelerated in an electrostatic accelerator. The degree of polarization, measured in Ref. [2], is ($36 \pm 2\%$) for 1.5 MeV neutrons.

The differential elastic scattering cross-sections for non-polarized neutrons were defined as the half-sums of the scattering cross-sections at the corresponding angles to the left and right of the incident neutron flux. From measurements of the angular distributions of the elastically scattered neutrons, the authors determined the total elastic scattering cross-sections, transport cross-sections and mean cosines of the elastic scattering angle. The measurement results were corrected for finite geometry and multiple scattering. The differential cross-sections are given in the form of a Legendre polynomial expansion:

$$\sigma(\vartheta) = \sum_{l=0}^{M} A_l P_l (\cos \vartheta)$$

Table I shows the calculated constants and coefficients A_l.

The polarizing power of the nuclei investigated is a complex function of the scattering angle and in absolute terms attains 10–20% in the majority of nuclei. The measured polarizing powers of the nuclei display no characteristic features in their behaviour as a function of the parity of the nuclear charge. The polarizing power values corrected for multiple scattering are shown in Table II.

Using an optical model of the nucleus, the authors analyse the experimental data on angular distributions of the scattered neutrons and the polarizing power of the nuclei studied. The theoretical calculations are based on a 6-parameter potential. The calculated data were adjusted to the experimental

results by the method of least squares with automatic variation of the potential parameters. The polarization calculations with parameters obtained by adjusting the theoretical to the experimental data for differential cross-sections do not tally with the experimental data on polarization for nuclei with $A < 60$. Inclusion of the polarization data in the analysis provides reliable information on spin-dependent nuclear forces. The total cross-sections calculated with the aid of the parameters obtained from adjustment to the differential cross-section and polarization data tally well with the experimental results. In the paper the authors discuss the dependence of the optical potential parameters on atomic weight.

REFERENCES

[1] KORZH, I.A. et al., Ukr. fiz. ž. 13 (1968) 1781.

[2] KELSEY, C.A., HOOP, B., Jr., VAN der MAAT, P., Nucl. Phys. 51 (1964) 395.

Table I

Coefficients for Legendre polynomial expansion of differential cross-sections. Total elastic scattering cross-sections, transport cross-sections and mean cosines of the elastic scattering angle

Element	A_0	A_1	A_2	A_3	A_4	A_5	σ_{el}, barn	σ_{trel}, barn	$\overline{\cos\theta}$
Fe	0,161	0,135	0,223	0,108	0,026	-0,004	2,024	1,458	0,279
Co	0,211	0,148	0,211	0,121	0,042	0,007	2,650	2,030	0,234
Ni	0,263	0,186	0,247	0,126	0,043	0,016	3,303	2,600	0,213
Cu	0,201	0,142	0,172	0,117	0,046	0,006	2,525	1,932	0,235
Zn	0,194	0,160	0,192	0,106	0,036	0,004	2,437	1,767	0,275
Zr	0,385	0,434	0,395	0,157	0,101	0,037	4,836	3,018	0,376
Nb	0,332	0,476	0,384	0,163	0,100	0,018	4,170	2,177	0,478
Mo	0,362	0,462	0,399	0,137	0,095	0,019	4,547	2,615	0,425

Table II

Polarizing power of nuclei for 1.5 MeV neutrons

ϑ Lab. co-ord syst.	$P_2(\theta)$				
	Ti	Cr	Fe	Co	Ni
20°	-(0,035±0,034)	-(0,029±0,019)	-(0,039±0,034)	-(0,039±0,034)	-(0,044±0,033)
30°	-(0,042±0,031)	-(0,039±0,025)	-(0,099±0,032)	-(0,069±0,030)	-(0,058±0,030)
40°	-(0,077±0,034)	-(0,055±0,024)	-(0,106±0,038)	-(0,053±0,021)	-(0,045±0,021)
55°	-(0,036±0,043)	-(0,054±0,033)	-(0,111±0,042)	-(0,055±0,038)	+(0,001±0,024)
70°	-(0,045±0,041)	-(0,074±0,032)	-(0,094±0,041)	+(0,050±0,035)	+(0,033±0,039)
85°	+(0,001±0,053)	-(0,008±0,032)	-(0,073±0,046)	+(0,037±0,037)	+(0,070±0,029)
100°	+(0,148±0,063)	+(0,073±0,036)	-(0,018±0,054)	+(0,016±0,033)	+(0,032±0,040)
115°	+(0,207±0,062)	+(0,051±0,034)	-(0,075±0,048)	+(0,013±0,034)	-(0,006±0,034)
130°	+(0,193±0,039)	+(0,088±0,031)	-(0,050±0,044)	+(0,019±0,034)	-(0,082±0,031)
145°	+(0,130±0,048)	+(0,053±0,033)	-(0,072±0,057)	-(0,017±0,048)	+(0,005±0,038)

ϑ Lab. co-ord. syst.	$P_2(\theta)$				
	Cu	Zn	Zr	Nb	Mo
20°	-(0,013±0,038)	-(0,032±0,034)	-(0,071±0,028)	-(0,065±0,027)	-(0,062±0,025)
30°	-(0,025±0,036)	-(0,045±0,031)	-(0,097±0,023)	-(0,091±0,028)	-(0,077±0,028)
40°	-(0,012±0,026)	+(0,010±0,030)	-(0,074±0,024)	-(0,076±0,034)	-(0,076±0,029)
55°	+(0,049±0,030)	+(0,044±0,034)	-(0,069±0,033)	-(0,064±0,035)	-(0,065±0,028)
70°	+(0,042±0,035)	+(0,073±0,032)	-(0,104±0,026)	-(0,022±0,037)	-(0,033±0,031)
85°	+(0,133±0,048)	+(0,137±0,037)	-(0,035±0,026)	-(0,044±0,040)	-(0,050±0,059)
100°	+(0,089±0,046)	+(0,062±0,039)	-(0,137±0,038)	-(0,052±0,057)	-(0,130±0,046)
115°	+(0,104±0,040)	+(0,042±0,046)	-(0,089±0,048)	+(0,029±0,061)	-(0,003±0,052)
130°	-(0,017±0,029)	+(0,030±0,048)	-(0,020±0,052)	+(0,074±0,090)	+(0,105±0,066)
145°	+(0,009±0,053)	-(0,027±0,054)	-(0,054±0,047)	+(0,220±0,081)	+(0,147±0,048)